BSc Thesis Applied Mathematics

Sensitivity Analysis of Elections for Dutch House of Commons (Tweede Kamer)

Shunzhe Zhang

Supervisor: Marie-Colette van Lieshout

June, 2026

Department of Applied Mathematics
Faculty of Electrical Engineering,
Mathematics and Computer Science

UNIVERSITY OF TWENTE.

Preface

This is the final project towards my Bachelor's degree in Applied Mathematics at the University of Twente. My interest in this area is because I have always had a passion with how the underlying mathematical structures would influence the real-world problems. By examining the total degree to which Tweede Kamer elections are affected by structural variables and stochastic uncertainties, I have attempted to provide a link between theoretical electoral models and the political reality they generate.

I am really thankful to my advisor, Marie-Colette van Lieshout for providing me with constructive guidance, patience, and thoughtful comments about this research project. Her support helped in creating an appropriate methodological framework and a completely mathematically sound study.

I am also thankful to the Department of Applied Mathematics for supplying the necessary resources. Most importantly, I want to thank my family and classmates for always supporting me during my undergraduate studies. I deeply appreciate the chance to conduct this research, and I hope to add a valuable mathematical view to the dialogue about fairness and stability in our elections.

Shunzhe Zhang
Enschede, June 2026

Sensitivity Analysis of Elections for Dutch House of Commons (Tweede Kamer)

Shunzhe Zhang*

June, 2026

Abstract

This thesis presents a comprehensive mathematical sensitivity analysis of the proportional representation (PR) system, as applied to the Dutch House of Commons (Tweede Kamer, hereinafter referred to as TK), focusing on the relationship between electoral fairness, party fragmentation, and seat-allocation stability. The study also examines how counting errors and voter uncertainty may affect vote distributions and final seat allocations. While existing studies often focus on deterministic measures of electoral fairness, this research uses a formal hybrid approach. By combining structural parameter analysis with the stochastic modeling of uncertainties using the 2025 Dutch Tweede Kamer (TK25) election data, this study provides a quantitative framework and theoretical foundation for evaluating electoral sensitivity.

First, dynamic threshold simulations (from 0.67% to 5.0%) and comparative analyses of six seat allocation algorithms reveal that the currently implemented D'Hondt method mathematically favors large parties. Additionally, the analysis identifies a sensitive instability interval between 1.8% and 2.7% in which the number of parliamentary parties changes sharply. Second, a probabilistic spatial counting error model is developed to evaluate the possibility of human error and how that affects the stability of seat distribution for major and minor political parties. The findings indicate that even if 10,000 ballots were misclassified, the corrected true error-free votes count would not have much impact on the final seat allocation compared to the official Dutch TK25 election results. The voter-transfer simulation shows that uncertainty mainly redistributes votes within ideologically related blocs. The centrist bloc is particularly affected. Finally, Ordinary Least Squares (OLS) regression analysis of TK23 to TK25 public opinion polls shows a linear decay in polling errors as the election day approaches. These results provide insights and suggestions for discussing the robustness of proportional representation under both structural and stochastic uncertainty.

Keywords: proportional representation, seat allocation, electoral thresholds, counting errors, voter uncertainty, opinion poll.

*Email: s.zhang-9@student.utwente.nl

Contents

1 Introduction

According to the Dutch Constitution, the Dutch House of Commons (TK) consists of 150 seats that are allocated based on proportional representation[23]. The key feature of this system is its low natural electoral threshold of 0.67%, meaning that a party can get a seat in parliament by receiving only 0.67% of the votes cast in the general election. This will also create many opportunities for political parties to be represented in parliament. While this low threshold allows multi-party representation, it also produces political instability and voter uncertainty, as voters cannot predict which alliance of parties will finally form a majority government[23]. For example, forming the Rutte IV cabinet in 2022 required 299 days, the longest government formation in Dutch history[23].

Typically, scholars evaluate seat allocation algorithms, such as the D'Hondt method used by the Dutch TK[9]. These studies typically rely on deterministic assumptions, such as assessing the large/small party bias[9]. It is also shown that the ultimate distribution of the remaining seats is influenced by practical, real-world uncertainty in addition to the structural parameters mentioned above[7][23]. In the context of the Dutch TK, which currently employs paper-based voting and manual vote counting in TK, there is a possibility that ballots could be misclassified due to physical sorting errors when counting votes after the election. Furthermore, voters often experience shifts in support to other ideologically similar parties in the weeks or so leading to the next general election.

Thus, evaluating the robustness of the Dutch TK electoral system based on these different variable models is essential. The primary research objective of this study is to analyze the effects of each of these variables on the voting and allocation processes used to assign seats in the Dutch TK, specifically from the perspective of how changes in both structural parameters and stochastic uncertainties will affect final seat allocations.

Based on this main research approach, the research is structured around five sub-research questions. First, based on a mathematical simulation of the Dutch TK25 results[26], this study evaluates how changes in the electoral threshold affect the degree of party fragmentation and the fairness of representation in the parliament. Second, under the same vote distribution, it compares the differences in fairness and stability when applying different seat allocation methods. Third, it investigates how the seat allocation results change if simulation errors in vote counting are introduced. Furthermore, it examines how voter uncertainty, modeled as stochastic vote transfers within and between ideological blocs, affects the stability of the Dutch TK25 seat allocation. Finally, it analyzes the volatility in voter preferences during the period from the Dutch TK23 to TK25 by studying the vote share data from opinion polls.

2 Related Work

The existing study of proportional representation systems has mainly focused on how votes are converted into seats. Different seats allocation methods and electoral thresholds may produce different outcomes of party's seats distribution in parliamentary under the same vote distribution. To compare such outcomes, the Gallagher Index is used to measure the imbalance between vote shares and seat shares [10], while the effective number of parties provides a way to measure party fragmentation at both the electoral and parliamentary aspects [19].

The second part of literature compares seat allocation methods within proportional representation. Divisor-based methods, in particular the D'Hondt method is known to give a relative advantage to larger parties[9]. By contrast, quota-based methods may reduce inequality in seat allocation. Van Eck, Visagie, and De Kock compared several seat allocation methods in proportional representation and show that the fairness of an allocation can be evaluated[7].

Electoral threshold is also an important mechanism. It is introduced to limit excessive party fragmentation, but it also produce wasted votes. Previous research shows that high threshold is an institutional tool used to reduce the number of parties entering parliament[5]. This creates a trade-off which is a higher threshold may simplify the formation of the government but reduce the fairness in elections. This trade-off is especially relevant for the Dutch TK where the natural threshold is low. Therefore, it is necessary to analyze threshold sensitivity.

However, the existing literature does not fully capture uncertainty in real elections. First, election process may occur counting and recording errors. Research on manual ballot counting and post-election audits shows that hand counting is a potential source of error[12]. Research on voting technologies also shows that the way votes are cast and counted can affect the number of uncounted or residual votes[3]. These findings motivate the counting-error model in this thesis.

Second, voter preferences are not fixed before election day. Aarts and Thomassen show that Dutch party competition can be described using several ideological dimensions[1]. Dutch voters are uncertain, but not completely random, many voters' intention change remain within ideologically coherent blocs[27]. This provides a justification for modelling voter uncertainty as stochastic vote transfers within and between ideological blocs rather than as fully random movement between all parties.

Third, volatility also appears in public opinion polling. Jennings and Wlezien analyze that polling errors evolve over the electoral timeline[15]. This motivates the regression analysis in this thesis, where polling error is modelled as a function of the number of days before the election.

3 Electoral Fragmentation and Fairness

To evaluate the impact of electoral rules on political outcomes, this study establishes an indicator framework using real election data from the Dutch TK25 to simulate the results. To specifically test the sensitivity of the system to threshold variations, the electoral threshold is incrementally adjusted from the current 0.67% up to 5.0%. These simulations apply the currently implemented D'Hondt method in Dutch TK, a highest averages algorithm that allocates seats iteratively by dividing each party's total votes by the sequence $1, 2, 3, \ldots$ and awarding the seat to the party with the largest current quotient[10].

Let $\mathcal{P} = \{1, 2, \ldots, n\}$ be the set of participating parties, $\mathcal{V}_i$ represent the percentage of votes received by party i, and $\mathcal{S}_i$ represent the percentage of seats allocated to that party. To assess the resulting electoral landscape across different simulations, the evaluation relies on three primary metrics. First, the Effective Number of Electoral Parties ($ENPV$)[19] measures the fragmentation of voter support among various parties during the voting stage of an election. Second, the Effective Number of Parliamentary Parties ($ENPP$)[19] measures the fragmentation of parties within the parliament after electoral results have been converted into seats. Finally, the Gallagher Index (LSq)[10] assesses the overall fairness and proportionality of the electoral system. The mathematical formulas and interpretations for these evaluation metrics are summarized in Table 1.

To analyze the impact of electoral thresholds on parliamentary outcomes, we conducted a sensitivity analysis by dynamically increasing the electoral threshold from the Dutch

Table 1: Indicators of electoral fragmentation and fairness.

Indicators	Formula	Trend	Status
$ENPV$	$\frac{1}{\sum_{i=1}^{n} \mathcal{V}_i^2}$	$\downarrow$	Concentrated
		$\uparrow$	Dispersed
$ENPP$	$\frac{1}{\sum_{i=1}^{n} \mathcal{S}_i^2}$	$\downarrow$	Concentrated
		$\uparrow$	Dispersed
LSq	$\sqrt{\frac{1}{2}\sum_{i=1}^{n}(\mathcal{V}_i - \mathcal{S}_i)^2}$	$\downarrow$	Fairer
		$\uparrow$	Unfair

baseline of 0.67% to a maximum of 5.0%. This simulation allows us to evaluate the trade-off between electoral fairness and parliamentary fragmentation.

3.1 Result of Sensitivity Analysis of Electoral Thresholds

In addition to calculating the indicators in Table 1, the number of political parties entering parliament was also added. The results, as illustrated in Figure 1, demonstrate the performance of the classical fairness-dispersion trade-off in proportional representation systems.

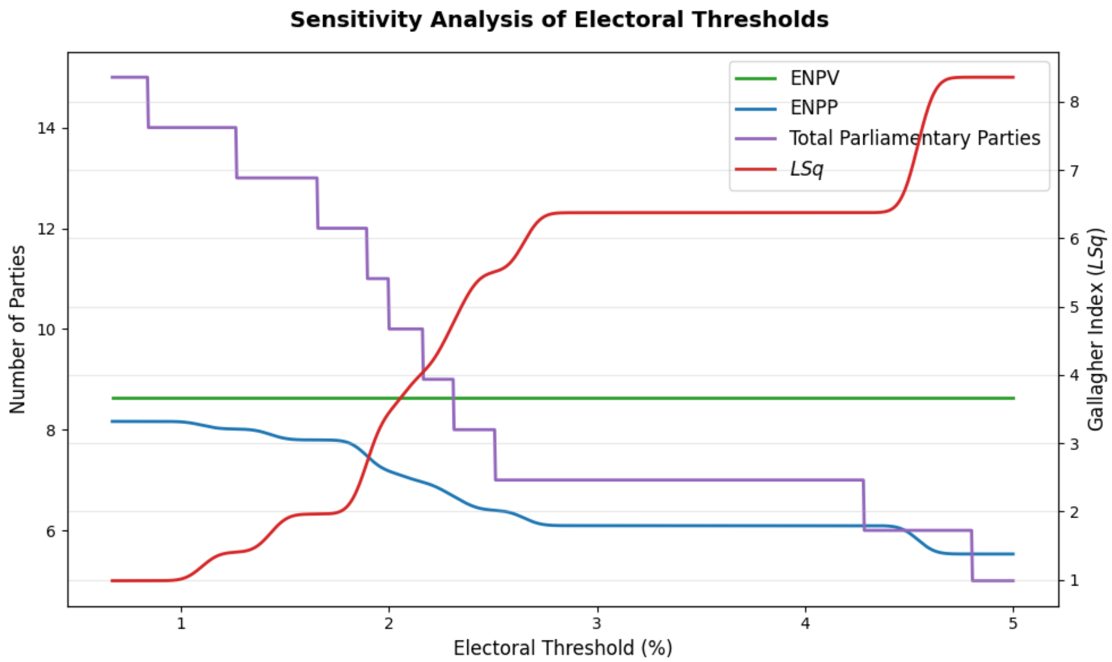

Figure 1: Fairness and party fragmentation across dynamic thresholds $[0.67\%, 5\%]$.

The Gallagher Index (LSq) shows a general upward trend, though this increase is punctuated by periods of stability where the index remains relatively flat. At the 0.67% baseline, the system is proportional, yielding an LSq of only 0.98. However, at a 5.0% threshold, the index surges to 8.36. As the threshold excludes more small parties, their accrued wasted votes are effectively removed from the initial pool. Consequently, the D'Hondt method redistributes these slack seats to larger parties, thereby reducing overall electoral fairness.

Since $ENPV$ is independent of thresholds, a higher electoral threshold does not change the true dispersion of voter preferences. Dutch voters' choices remain dispersed. Even if some smaller parties are unable to enter parliament due to the higher threshold, they still have a base of support at the voter level. $ENPP$ shows a consistent downward trend as the electoral threshold increases, characterized by a distinct step-wise decline. At the baseline threshold of 0.67%, the parliament shows high fragmentation with 8.16 effective parties. As the threshold increases, the reduction in the number of effective parties does not follow a linear trajectory but rather a step-wise function. At the maximum simulated threshold of 5.0%, effective number of parties is decrease to 5.53 parties. The total number of parliamentary parties displays a more pronounced step-wise pattern, decreasing from 15 parties at the baseline threshold to 5 parties at the 5.0% threshold.

A sensitive interval is observed between 1.8% and 2.7%. During this interval, the number of parliamentary parties drops from 13 to 7, while $ENPP$ decreases from 7.75 to 6.16. There has been no significant change in the effective political parties.

4 Mathematical Framework of Seat Allocation Algorithms

In proportional representation systems, translating votes into seats relies on specific mathematical allocation mechanisms. Different algorithms, such as divisor and quota methods, operate under distinct mathematical rules that inherently reflect different political priorities, deciding whether a system favors large-party stability or proportional fairness[24].

Within divisor method, the D'Hondt method uses a sequential divisor sequence, serving as the current electoral standard in the Netherlands. The Sainte-Laguë method employs an odd-number divisor sequence. The Modified Sainte-Laguë method alters the first divisor to 1.4, as a barrier to entry.

Quota methods, on the other hand, distribute seats based on a specific electoral quota. Their performance depends on the size of the chosen denominator. The Hare Quota uses a simple mathematical average, resulting in high proportionality but often leaving a large number of slack seats for the second phase. The Droop Quota slightly lowers the denominator and additional seat was added. Finally, the Imperiali Quota uses an even smaller denominator, minimize overall slack seats.

With a fixed threshold of 0.67% and dynamic thresholds [0.67%, 5%], this section tests the robustness of election outcomes against six allocation methods: three highest averages (divisor) methods and three largest remainder (quota) methods. Let V_i denote the valid votes for party i, and $V_{total} = \sum_{i=1}^{n} V_i$ be the total valid votes. The total parliamentary seats are fixed at $S = 150$. To compare these algorithms, both diviosr and quota methods are structured into a two-phase procedural framework: Phase 1 (Baseline) and Phase 2 (Slack). The indicators summarized in Table 1 will be used again to assess their performance.

4.1 Highest Averages Methods (Divisor Methods)

These methods allocate seats iteratively based on the highest average votes per seat. In practice, this is executed in two phases to optimize the allocation process.

Phase 1: Baseline Allocation. A standard quota $Q = V_{total}/S$ is used to establish the baseline. To guarantee that the allocated seats are integer numbers, each party receives an integer baseline number of seats by applying the floor function:

$$s_{base,i} = \lfloor \frac{V_i}{Q} \rfloor$$

The absolute number of seats currently allocated to party i is initialized as $s_i = s_{base,i}$.

Phase 2: Slack Allocation. The unallocated slack seats, calculated as the integer $S_{slack} = S - \sum s_{base,i}$, are distributed iteratively. In each iteration, a quotient Q_i is calculated based on the total votes V_i and the seats s_i already allocated. The party with the highest Q_i receives one seat, incrementing its s_i by 1, until all S_{slack} seats are assigned.

The methods differ solely by their divisor sequences. Specifically, the D'Hondt method[10] uses a sequential divisor sequence of $1, 2, 3, \ldots$, where the quotient is calculated as:

$$Q_i = \frac{V_i}{s_i + 1}.$$

In contrast, the Sainte-Laguë method[25] uses odd numbers $1, 3, 5, \ldots$, with the quotient defined as:

$$Q_i = \frac{V_i}{2s_i + 1}.$$

Furthermore, the (Modified) Sainte-Laguë method[25] modifies the first divisor to 1.4, the quotient is calculated conditionally:

$$Q_i = \begin{cases} \frac{V_i}{1.4} & \text{if } s_i = 0 \\ \frac{V_i}{2s_i+1} & \text{if } s_i > 0 \end{cases}.$$

4.2 Largest Remainder Methods (Quota Methods)

These methods distribute seats based on a specific electoral quota. Similar to divisor methods, this process is executed in two distinct phases.

Phase 1: Baseline Allocation. An electoral quota Q is determined based on the specific method applied. To ensure validity, each party receives a baseline number of seats equal to the integer division of their votes by this quota, defined using the floor function:

$$s_{base,i} = \lfloor \frac{V_i}{Q} \rfloor.$$

The algorithms differ based on the initial quota Q applied, which directly influences their political proportionality. The Hare Quota[24] uses a simple, unbiased quota defined as:

$$Q_{Hare} = \frac{V_{total}}{S}.$$

This approach provides the most straightforward proportional representation, leaves a large number of slack seats unallocated for the second phase. The Droop Quota[24] uses a slightly smaller quota:

$$Q_{Droop} = \lfloor \frac{V_{total}}{S + 1} \rfloor + 1.$$

This modification accelerates the initial allocation phase, which practically advantages medium to larger parties compared to the Hare method. Lastly, the Imperiali Quota[24] uses an even smaller quota:

$$Q_{Imperiali} = \frac{V_{total}}{S + 2}.$$

This is designed to reward large parties during the initial allocation phase and minimize the overall number of slack seats.

Phase 2: Slack Allocation. The remaining integer unallocated seats, calculated as $S_{slack} = S - \sum s_{base,i}$, are distributed one by one. The remainder for each party is evaluated as:

$$R_i = \frac{V_i}{Q} - s_{base,i} \ ,$$

where this remainder value exists within the fractional space $R_i \in [0, 1)$. All participating parties are then ranked in descending order based on their R_i values. The S_{slack} unallocated seats are distributed by assigning exactly one additional seat to each of the top S_{slack} parties in this ranking, until all remaining seats are assigned.

4.3 Result

4.3.1 Seats Distribution Analysis of Divisor and Quota Methods

In Figure 2, we apply six different seat allocation methods to the Dutch TK25 election data with the same threshold of 0.67%. In addition, to make it more intuitive to analyze the differences between different seat allocation methods, we will display the initial allocated seats and the slack seats separately. Minimum number of political parties to form a government (≥ 76 seats) and total number parties of entering the parliament were used for comparison, under the same threshold 0.67%.

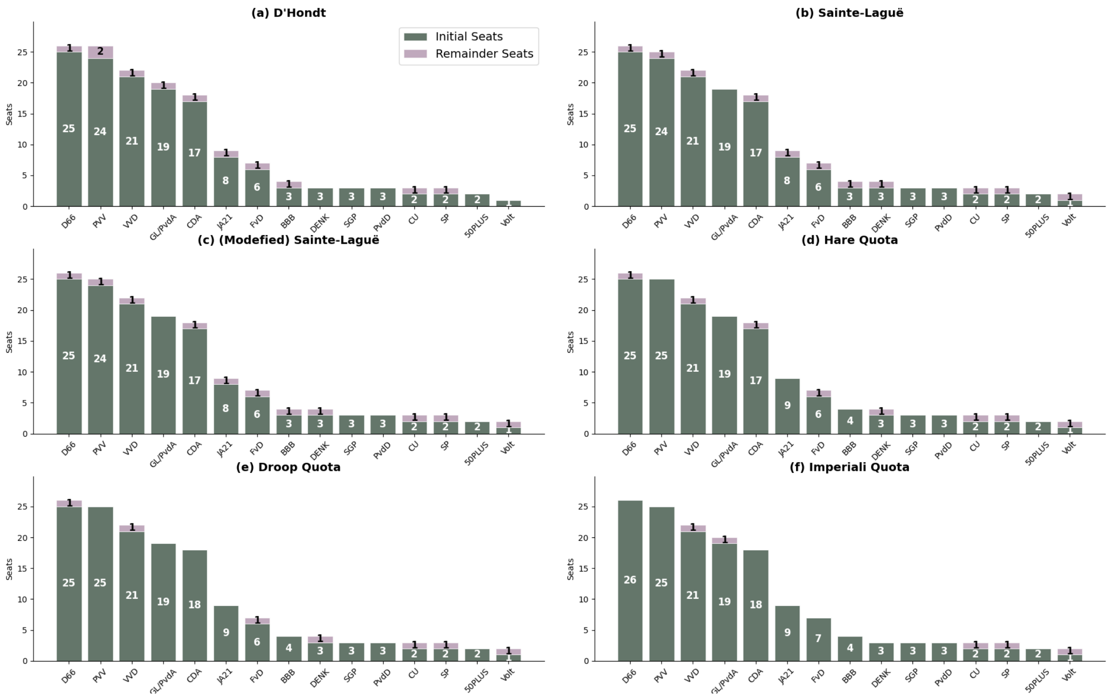

FIGURE 2: Seat allocation results for three divisor methods and three quota methods with 0.67% threshold.

Figure 2(a), the currently implemented D'Hondt method in the Netherlands, shows a preference for larger parties. By decomposing the total seats into initial seats and slack seats, the internal mechanics of the D'Hondt algorithm become visible. It reduces the number of slack seats won by smaller parties (Volt's number of seats dropped from 2 to 1) and allocates those slack seats up to larger parties (e.g., PVV gained 2 remaining seats). The final seat distributions in Figure 2(b) and Figure 2(c) are entirely identical. The (Modified) Sainte-Laguë method was originally designed to penalize micro-parties by setting the first divisor to 1.4. However, because the 0.67% electoral threshold acts as an initial filter. All 15 qualified parties have a sufficient vote base to avoid this penalty. Consequently, the penalty mechanism fails, and the algorithm functionally regresses to the standard Sainte-Laguë method.

Figure 2(d) and Figure 2(e) show an unbiased distribution under the same threshold. The Hare quota generates a larger number of 8 slack seats, distributing them among small and medium parties. Although the Droop quota utilizes a slightly smaller number of slack seats, the total number of seats of each party's is exactly the same. The only difference between them is the ratio of initial and slack seats (e.g., CDA in Figure 2(d) is 17 initial with 1 slack seat, while CDA in Figure 2(e) is 18 initial with 0 slack seats), but the final total number of seats is the same. Figure 2(f) presents the most extreme slack seats distribution pattern, and the smallest number of 5 slack seats, compared with the previous two algorithms. The Imperiali quota rewards large parties during the initial seat allocation phase. For instance, D66 receives 26 initial seats, which reduces the slack seats available for smaller parties right from the initial allocation stage.

TABLE 2: Comparison of allocation methods with 0.67% threshold

Method	S_{inital}	S_{slack}	LSq	N_{gov}	N_{final}
D'Hondt	139	11	0.9849	4	15
Sainte-Laguë	139	11	0.7143	4	15
(Modified) Sainte-Laguë	139	11	0.7143	4	15
Hare	142	8	0.7143	4	15
Droop	143	7	0.7143	4	15
Imperiali	145	5	0.8207	4	15

Table 2 provides a quantitative evaluation across the six allocation methods under the 0.67% threshold. To comprehensively assess these methods, we evaluate five specific indicators: the number of initial seats ($S_{initial}$), the number of slack seats (S_{slack}), the Gallagher Index (LSq), the minimum number of parties required to form a majority government (N_{gov}), and the final number of parliamentary parties (N_{final}).

Regarding divisor methods, all three methods generate an identical division of 139 initial seats and 11 slack seats. This indicates that 11 seats remain, determined purely by the comparison of highest averages. Regarding quota methods, as the quota denominator decreases across these methods, the system allocates more initial seats ($S_{initial}$), leading to a reduction in slack seats (S_{slack}). The slack seats drop from 8 under Hare, to 7 under Droop, and plunge to merely 5 under Imperiali.

Sainte-Laguë and (Modified) Sainte-Laguë methods distribute 11 slack seats evenly among smaller parties, achieving a high degree of proportional fairness ($LSq = 0.7143$). The D'Hondt method prioritizes awarding the 11 slack seats to the leading party, thus reducing fairness ($LSq = 0.9849$). This proves that the currently implemented D'Hondt in the Dutch TK favors larger political parties.

Despite the differences in $S_{initial}$, S_{slack}, and LSq across the algorithms, the metrics measuring political stability remain the same. Regardless of the allocation method employed, the final number of parliament parties (N_{final}) remains locked at 15, and the minimum number of parties required to form a majority government (N_{gov}) is consistently 4. This robust finding demonstrates that attempting to ease coalition formation by only changing the mathematical allocation algorithm is ineffective.

4.3.2 Threshold Sensitivity Analysis of Divisor and Quota Methods

We also extend the threshold sensitivity analysis introduced in Section 3 to six seat allocation methods and compare their respective outcomes. The results are shown in Figure 3.

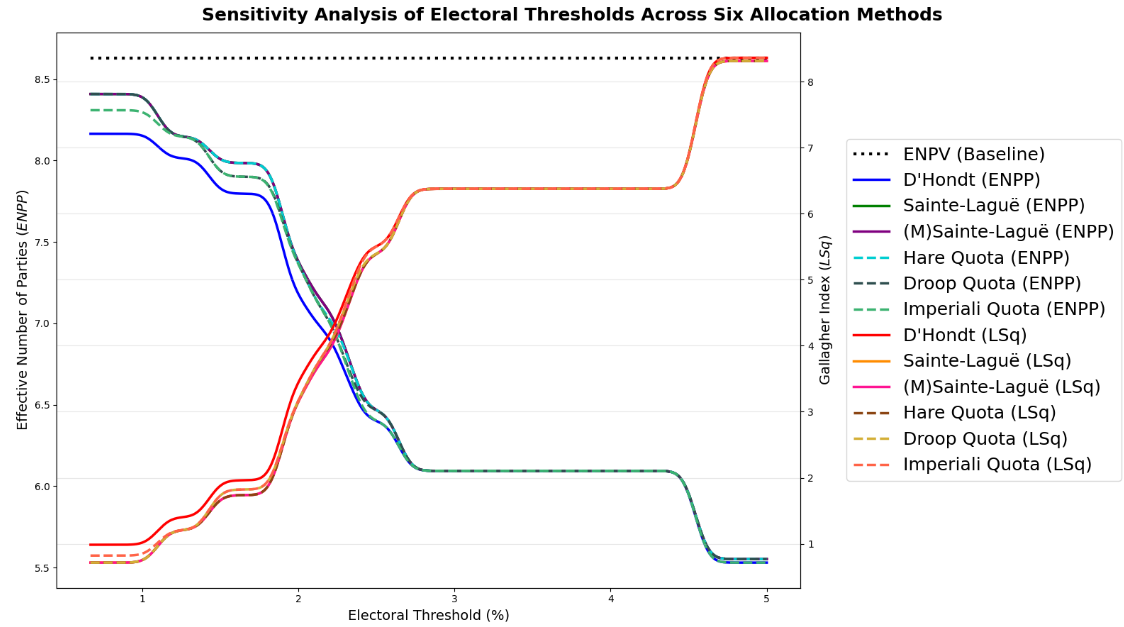

FIGURE 3: Seat allocation results for divisor and quota methods with dynamic thresholds $[0.67\%, 5\%]$.

The horizontal black dotted line at the top of Figure 3 is $ENPV$. $ENPV$ is independent of the threshold, therefore a change of algorithm will not affect the dispersion of electoral parties in the Netherlands, which remains relatively dispersed.

Second, under the low threshold ($\leq 1.8\%$), the D'Hondt and Imperiali methods yield the lowest $ENPP$ and the highest LSq. Specifically, the D'Hondt method has the highest degree of parliamentary concentration, followed by Imperiali method, while other methods are relatively more dispersed. Conversely, the Sainte-Laguë, (Modified) Sainte-Laguë, Hare and Droop methods are the fairest, followed by the Imperiali method. In comparison, the D'Hondt method shows the most unfairness.

As the electoral threshold gradually increases, particularly after crossing 2.7%, all algorithm curves converge and finally overlap. As the electoral threshold increases, the impact of seat allocation algorithms on parliament gradually become small, particularly regarding the effectiveness of political parties and fairness within the parliament. When the electoral threshold is sufficiently high, differences in algorithms have almost no effect on parliament.

However, even as the rising threshold causes the different allocation methods to converge, the overall parliament remains fragmented. Furthermore, regardless of the specific algorithmic variations, the electoral outcome remains at a relatively high level.

5 Counting Error Model

The choice of electoral recording mechanisms involves a fundamental trade-off between cyber-security and operational accuracy. While electronic systems offer efficiency, they are susceptible to malicious digital interference. Conversely, manual paper-and-pencil recording, as implemented in the Netherlands, enhances transparency and mitigates the risk of large-scale cyber-manipulation. However, this paper-based approach is inherently vulnerable to stochastic physical misclassification and human error.

To prevent cyber-manipulation, the Netherlands abolished electronic voting in 2017[6], reverting to manual paper-and-pencil recording. Voters use a red pencil to fill in a circle next to a candidate's name on a large ballot paper (see Figure 4). Staff categorize ballots by party, record totals at each polling station, and transport results to the municipal electoral office for municipal reporting and aggregation[18]. Final compilation is performed by the Central Electoral Commission (Kiesraad) in The Hague[18].

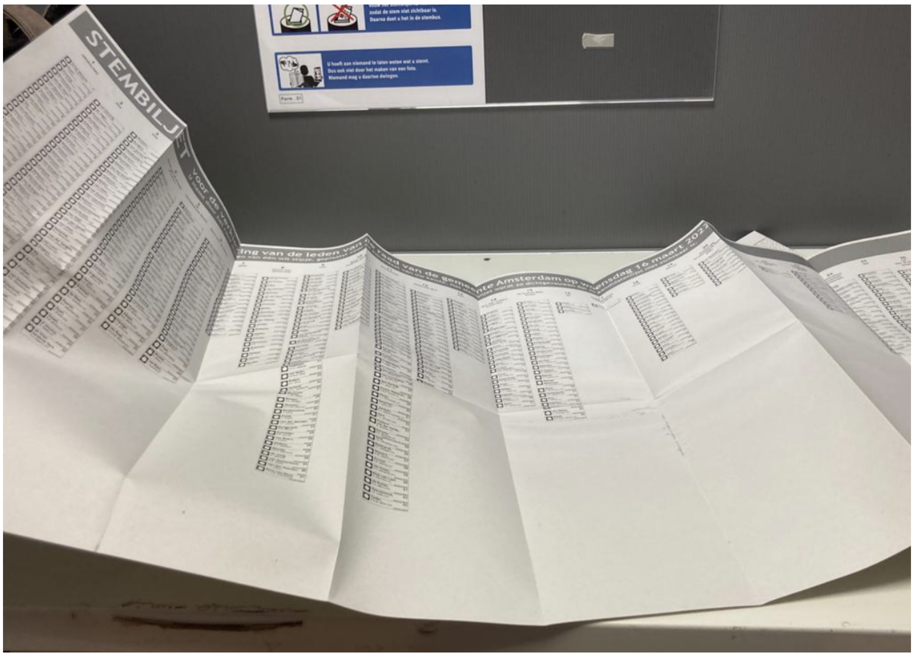

FIGURE 4: Large Dutch Tweede Kamer ballot paper[22].

5.1 Physical Model of Counting Errors

In large-scale paper-based electoral systems, the vote-counting process is often affected by physical misalignment. To quantify the potential impact on the final parliamentary seat allocation, this study establishes a misclassification model based on physical proximity on the ballot paper.

Let $n \in \mathbb{N}$ denote the total number of political parties participating in the election, ordered sequentially according to the ballot paper, i.e. $\mathcal{P} = \{1, 2, \ldots, n\}$. We define two $(n+2)$-dimensional vectors to characterize the voting state. The first n components correspond to valid party votes, while the last two components correspond to blank and invalid ballots.

- Real(error-free) voting vector: $X = [X_{\mathcal{P}}, x_B, x_I]^T \in \mathbb{Z}_{\geq 0}^{n+2}$ where $X_{\mathcal{P}} = [x_1, x_2, \ldots, x_n]^T \in \mathbb{Z}_{\geq 0}^{n}$.
- Observed(official) voting vector: $Y = [Y_{\mathcal{P}}, y_B, y_I]^T \in \mathbb{Z}_{\geq 0}^{n+2}$ where $Y_{\mathcal{P}} = [y_1, y_2, \ldots, y_n]^T \in \mathbb{Z}_{\geq 0}^{n}$.

For valid party votes, based on the structural design of physical ballots (see Figure 4), the probability of a valid party vote being misclassified depends on its spatial positioning relative to neighboring parties. In addition, a valid party vote may also be misjudged as blank or invalid ballot.

For blank ballots, there is a low probability that a blank ballot will be incorrectly assigned to either a valid or invalid ballot. Conversely, there is also a certain probability that an invalid ballot will be incorrectly assigned to either a valid or blank ballot. Hence, The model is formed under the following assumptions:

- **Misclassification Rate:**
  For valid party votes, let $\epsilon \in [0, 1]$ be the total misclassification rate, which decomposes into three mutually exclusive error outcomes: $\epsilon = \epsilon_{\mathcal{P}} + \epsilon_B + \epsilon_I$, where:

$$\epsilon := \begin{cases} \epsilon_{\mathcal{P}} : \text{valid party vote} \to \text{neighbouring party} \\ \epsilon_B : \text{valid party vote} \to \text{blank} \\ \epsilon_I : \text{valid party vote} \to \text{invalid} \end{cases}$$

  For blank votes, let $\zeta \in [0, 1]$ be the total misclassification rate, which decomposes into two mutually exclusive error outcomes: $\zeta = \zeta_{\mathcal{P}} + \zeta_I$, where:

$$\zeta := \begin{cases} \zeta_{\mathcal{P}} : \text{blank} \to \text{valid party vote} \\ \zeta_I : \text{blank} \to \text{invalid} \end{cases}$$

  For invalid votes, let $\eta \in [0, 1]$ be the total misclassification rate, which decomposes into two mutually exclusive error outcomes: $\eta = \eta_{\mathcal{P}} + \eta_B$, where:

$$\eta := \begin{cases} \eta_{\mathcal{P}} : \text{invalid} \to \text{valid party vote} \\ \eta_B : \text{invalid} \to \text{blank} \end{cases}$$

- **Spatially Transfer:** We define the transfer probability $p_j \in [0, 1]$, where $j \in \mathcal{P}$. That is, the probability of the vote of party j shifting to the left is p_j, the probability of shifting to the right is $1 - p_j$. A party located at the physical margins of the ballot paper can only be shifted to its adjacent party, i.e. $p_1 = 0$ and $p_n = 1$.

5.2 Misclassification Probability Distribution

For a single valid ballot originally cast for party j (where $j \in \mathcal{P}$), let $E_{\mathcal{P},j}$ denote the event that a spatial counting error occurs, misclassifying this specific ballot to an adjacent party. We assume this baseline error rate is independent of the specific party, thus $P(E_{\mathcal{P},j}) = \epsilon_{\mathcal{P}}$.

Let L and R denote the mutually exclusive spatial events of this ballot shifting to its left neighbor and right neighbor, respectively. The spatial shift parameter p_j is defined as the conditional probability of a leftward shift, given that a spatial error has already occurred for party j's ballot:

$$P(L \mid E_{\mathcal{P},j}) = p_j, \quad P(R \mid E_{\mathcal{P},j}) = 1 - p_j,$$

According to Bayes' Theorem, the joint probability that a ballot cast for party j is both misclassified and shifted to the left (or right) neighbor is given by:

$$P(L \cap E_{\mathcal{P},j}) = P(E_{\mathcal{P},j}) \cdot P(L \mid E_{\mathcal{P},j}) = \epsilon_{\mathcal{P}} \cdot p_j$$

$$P(R \cap E_{\mathcal{P},j}) = P(E_{\mathcal{P},j}) \cdot P(R \mid E_{\mathcal{P},j}) = \epsilon_{\mathcal{P}} \cdot (1 - p_j)$$

Let $\mathbf{V}^{(j)}$ be the random vector representing the final destinations of the x_j independent true votes of party j. Since each voter makes their decision independently, we introduce the true vote count x_j as the parameter for the number of independent trials. For any party, the vote flow diverges into five mutually exclusive outcome categories: shifting to the left, right, blank, invalid, or being correctly retained. The random vector follows a Multinomial distribution:

$$\begin{pmatrix} V_{j\to j-1} \\ V_{j\to j} \\ V_{j\to j+1} \\ V_{j\to B} \\ V_{j\to I} \end{pmatrix} \sim \text{Multinomial}\left(x_j, \begin{bmatrix} \epsilon_{\mathcal{P}} \cdot p_j \\ 1-\epsilon \\ \epsilon_{\mathcal{P}} \cdot (1-p_j) \\ \epsilon_B \\ \epsilon_I \end{bmatrix} \right).$$

We define the true weight of each party as: $w_j = \frac{x_j}{\sum_{j=1}^n x_j}$, and $\sum_{j=1}^n w_j = 1$. Similar to the argument that derives $\mathbf{V}^{(j)}$, let $\mathbf{V}^{(B)}$ be the random vector representing the final destinations of the x_B and let $\mathbf{V}^{(I)}$ be the random vector representing the final destinations of the x_I. Using the true counts x_B and x_I as the trial parameters for blank and invalid votes respectively. We derive their distribution as follows:

$$\begin{pmatrix} V_{B\to 1} \\ \vdots \\ V_{B\to n} \\ V_{B\to B} \\ V_{B\to I} \end{pmatrix} \sim \text{Multinomial}\left(x_B, \begin{bmatrix} \zeta_{\mathcal{P}} \cdot w_1 \\ \vdots \\ \zeta_{\mathcal{P}} \cdot w_n \\ 1-\zeta \\ \zeta_I \end{bmatrix} \right),$$

$$\begin{pmatrix} V_{I\to 1} \\ \vdots \\ V_{I\to n} \\ V_{I\to B} \\ V_{I\to I} \end{pmatrix} \sim \text{Multinomial}\left(x_I, \begin{bmatrix} \eta_{\mathcal{P}} \cdot w_1 \\ \vdots \\ \eta_{\mathcal{P}} \cdot w_n \\ \eta_B \\ 1-\eta \end{bmatrix} \right).$$

5.3 Construct the Confidence Interval of Real Voting Data

In this subsection, we aim to construct confidence intervals for the true vote counts X based on the official observed counts Y. To achieve this, we first derive an estimator for X by calculating the expected values of the marginal distributions. Subsequently, we determine the variance and covariance of these estimators, allowing us to apply the Central Limit Theorem to establish the final confidence intervals

Estimation of Real Voting Data X

By the properties of the Multinomial distribution, the marginal distribution of each component in $V_{(\cdot)}$ follows a Binomial distribution with parameters $(x_{(\cdot)}, p_{(\cdot)})$. For any party j, its expected observed vote count $E[y_i]$, is constructed from the sum of five independent components for any party $j \in \{1, 2, \ldots, n\}$:

$$E[y_j] = E[V_{j-1\to j}] + E[V_{j\to j}] + E[V_{j+1\to j}] + E[V_{B\to j}] + E[V_{I\to j}]$$

$$E[y_j] = \underbrace{\epsilon_{\mathcal{P}}(1-p_{i-1})x_{j-1}}_{\substack{\text{inflow from} \\ \text{party } (j-1)}} + \underbrace{(1-\epsilon)x_j}_{\substack{\text{true votes} \\ \text{retained by} \\ \text{party } (j)}} + \underbrace{\epsilon_{\mathcal{P}} p_{j+1} x_{j+1}}_{\substack{\text{inflow from} \\ \text{party } (j+1)}} + \underbrace{\zeta_{\mathcal{P}} w_j x_B}_{\substack{\text{inflow from} \\ \text{blank}}} + \underbrace{\eta_{\mathcal{P}} w_j x_I}_{\substack{\text{inflow from} \\ \text{invalid}}} \tag{1}$$

To handle the boundary cases at the ends of the ballot paper consistently within the generalized expectation formula, we define the variables $x_0 = 0$ and $x_{n+1} = 0$. By applying this decomposition logic across blank and invalid parts, we derive the expected observed vote count for blank and invalid as below:

$$E[y_B] = \underbrace{\epsilon_B \sum_{j=1}^{n} x_j}_{\text{inflow from each party}} + \underbrace{(1-\zeta)x_B}_{\text{true votes retained by blank}} + \underbrace{\eta_B x_I}_{\text{inflow from invalid}} \tag{2}$$

$$E[y_I] = \underbrace{\epsilon_I \sum_{j=1}^{n} x_j}_{\text{inflow from each party}} + \underbrace{(1-\eta)x_I}_{\text{true votes retained by invalid}} + \underbrace{\zeta_I x_B}_{\text{inflow from blank}} \tag{3}$$

Combine Equation 1, 2, 3, and write them in matrix form $E[Y] = T(X)X$:

$$\begin{bmatrix} E[y_1] \\ E[y_2] \\ E[y_3] \\ \vdots \\ E[y_{n-1}] \\ E[y_n] \\ E[y_B] \\ E[y_I] \end{bmatrix} = \left[\begin{array}{cccccc|cc} 1-\epsilon & \epsilon_{\mathcal{P}} p_2 & 0 & \dots & 0 & 0 & \zeta_{\mathcal{P}} w_1 & \eta_{\mathcal{P}} w_1 \\ \epsilon_{\mathcal{P}} & 1-\epsilon & \epsilon_{\mathcal{P}} p_3 & \dots & 0 & 0 & \zeta_{\mathcal{P}} w_2 & \eta_{\mathcal{P}} w_2 \\ 0 & \epsilon_{\mathcal{P}}(1-p_2) & 1-\epsilon & \dots & 0 & 0 & \zeta_{\mathcal{P}} w_3 & \eta_{\mathcal{P}} w_3 \\ \vdots & \vdots & \vdots & \ddots & \vdots & \vdots & \vdots & \vdots \\ 0 & 0 & 0 & \dots & 1-\epsilon & \epsilon_{\mathcal{P}} & \zeta_{\mathcal{P}} w_{n-1} & \eta_{\mathcal{P}} w_{n-1} \\ 0 & 0 & 0 & \dots & \epsilon_{\mathcal{P}}(1-p_{n-1}) & 1-\epsilon & \zeta_{\mathcal{P}} w_n & \eta_{\mathcal{P}} w_n \\ \hline \epsilon_B & \epsilon_B & \epsilon_B & \dots & \epsilon_B & \epsilon_B & 1-\zeta & \eta_B \\ \epsilon_I & \epsilon_I & \epsilon_I & \dots & \epsilon_I & \epsilon_I & \zeta_I & 1-\eta \end{array}\right] \begin{bmatrix} x_1 \\ x_2 \\ x_3 \\ \vdots \\ x_{n-1} \\ x_n \\ x_B \\ x_I \end{bmatrix} \tag{4}$$

Separation of Variables

Consider the matrix form of Equation 4 $E[Y] = T(X)X$, where $T(X)_{(n+2)\times(n+2)}$ is the transition matrix. $T(X)$ is dependent on the true voting vector X due to the true weight parameters w_j. Due to the introduction of nonlinearity, we cannot directly solve the estimator $\widehat{X} = T(X)^{-1}E(Y)$. Therefore, we need to separate the variable X from $T(X)$.

Firstly, we define the sum of the true votes of valid parties as $V_{total(x)} = \sum_{j=1}^{n} x_j$, and the sum of the expected observed votes of valid parties as $V_{total(y)} = \sum_{j=1}^{n} E[y_j]$. Replace $E[y_j]$ with Equation 1 for $j \in \{1, 2, \dots, n\}$, we get:

$$V_{total(y)} = (\sum_{j=1}^{n} \epsilon_{\mathcal{P}}(1-p_{j-1})x_{j-1} + \sum_{j=1}^{n} \epsilon_{\mathcal{P}} p_{j+1} x_{j+1}) + \sum_{j=1}^{n}(1-\epsilon)x_j + (\sum_{j=1}^{n} \zeta_{\mathcal{P}} w_j x_B + \sum_{j=1}^{n} \eta_{\mathcal{P}} w_j x_I)$$

Consider the first component, let $k = j-1$ and $l = j+1$. Recall that $\sum_{j=1}^{n} w_j = 1$, so we have:

$$V_{total(y)} = (\epsilon_{\mathcal{P}} \sum_{k=0}^{n-1}(1-p_k)x_k + \epsilon_{\mathcal{P}} \sum_{l=2}^{n+1} p_l x_l) + (1-\epsilon)V_{total(x)} + (\zeta_{\mathcal{P}} x_B + \eta_{\mathcal{P}} x_I)$$

Substitute the boundary condition $x_0 = x_{n+1} = 0$, $p_1 = 0$ and $p_n = 1$ into the first component, so we have:

$$V_{total(y)} = (\epsilon_{\mathcal{P}} \sum_{k=1}^{n}(1-p_k)x_k + \epsilon_{\mathcal{P}} \sum_{l=1}^{n} p_l x_l) + (1-\epsilon)V_{total(x)} + (\zeta_{\mathcal{P}} x_B + \eta_{\mathcal{P}} x_I)$$

Now we can let $k = l$:

$$\begin{aligned} V_{total(y)} &= \epsilon_{\mathcal{P}} \sum_{k=1}^{n} (1 - p_k + p_k) x_k + (1-\epsilon) V_{total(x)} + \zeta_{\mathcal{P}} x_B + \eta_{\mathcal{P}} x_I \\ &= \epsilon_{\mathcal{P}} V_{total(x)} + (1-\epsilon) V_{total(x)} + \zeta_{\mathcal{P}} x_B + \eta_{\mathcal{P}} x_I \end{aligned}$$

Recall that $\epsilon = \epsilon_{\mathcal{P}} + \epsilon_B + \epsilon_I$, then finally we derive $V_{total(y)}$:

$$V_{total(y)} = (1 - \epsilon_B - \epsilon_I) V_{total(x)} + \zeta_{\mathcal{P}} x_B + \eta_{\mathcal{P}} x_I \tag{5}$$

Combine Equation 2, 3, 5, and we write them in matrix form:

$$\begin{bmatrix} V_{total(y)} \\ E[y_B] \\ E[y_I] \end{bmatrix} = \begin{bmatrix} 1 - \epsilon_B - \epsilon_I & \zeta_{\mathcal{P}} & \eta_{\mathcal{P}} \\ \epsilon_B & 1 - \zeta & \eta_B \\ \epsilon_I & \zeta_I & 1 - \eta \end{bmatrix} \begin{bmatrix} V_{total(x)} \\ x_B \\ x_I \end{bmatrix} \tag{6}$$

By applying the method of moments, we equate the expected values to the observed data ($E[y_B] = y_B$ and $E[y_I] = y_I$). Furthermore, while y_B and y_I are direct observations, $V_{total(y)}$ is computed as the sum of all observed valid party votes. With these substitutions, we can invert this 3×3 matrix to solve for the estimators $[\hat{V}_{total(x)}, \hat{x}_B, \hat{x}_I]^T$ from Equation 6.

Since the inflow terms for blank and invalid votes in Equation 1 are $\zeta_{\mathcal{P}} w_j x_B$ and $\eta_{\mathcal{P}} w_j x_I$, and recall that $w_j = \frac{x_j}{\sum_{j=1}^{n} x_j}$. At this stage, the true vote count for each party x_j is still unknown and is exactly what we are trying to solve for. However, since we have already derived the estimated values $\hat{V}_{total(x)}$, $\hat{x}_B$, and $\hat{x}_I$, we can plug these known estimators into the formula. This allows us to extract x_j and transform the inflow terms of blank and invalid into:

$$\zeta_{\mathcal{P}} w_j x_B + \eta_{\mathcal{P}} w_j x_I = \frac{x_j}{\sum_{j=1}^{n} x_j} (\zeta_{\mathcal{P}} x_B + \eta_{\mathcal{P}} x_I) = x_j \left(\frac{\zeta_{\mathcal{P}} \hat{x}_B + \eta_{\mathcal{P}} \hat{x}_I}{\hat{V}_{total(x)}} \right)$$

Define a blank and invalid inflow constant C:

$$C = \frac{\zeta_{\mathcal{P}} \hat{x}_B + \eta_{\mathcal{P}} \hat{x}_I}{\hat{V}_{total(x)}}$$

Substitute C back into Equation 1, we get:

$$E[y_j] = \epsilon_{\mathcal{P}} (1 - p_{j-1}) x_{j-1} + (1 - \epsilon + C) x_j + \epsilon_{\mathcal{P}} p_{j+1} x_{j+1} \tag{7}$$

Now the nonlinearity has been eliminated. We can write Equation 7 in matrix form $E[Y_{\mathcal{P}}] = \widehat{M} X_{\mathcal{P}}$, where $\widehat{M}_{n \times n}$ is the reduced linear estimation matrix:

$$\begin{bmatrix} E[y_1] \\ E[y_2] \\ E[y_3] \\ \vdots \\ E[y_{n-1}] \\ E[y_n] \end{bmatrix} = \begin{bmatrix} 1-\epsilon+C & \epsilon_{\mathcal{P}} p_2 & 0 & \dots & 0 & 0 \\ \epsilon_{\mathcal{P}} & 1-\epsilon+C & \epsilon_{\mathcal{P}} p_3 & \dots & 0 & 0 \\ 0 & \epsilon_{\mathcal{P}}(1-p_2) & 1-\epsilon+C & \dots & 0 & 0 \\ \vdots & \vdots & \vdots & \ddots & \vdots & \vdots \\ 0 & 0 & 0 & \dots & 1-\epsilon+C & \epsilon_{\mathcal{P}} \\ 0 & 0 & 0 & \dots & \epsilon_{\mathcal{P}}(1-p_{n-1}) & 1-\epsilon+C \end{bmatrix} \begin{bmatrix} x_1 \\ x_2 \\ x_3 \\ \vdots \\ x_{n-1} \\ x_n \end{bmatrix}$$

Hence we can finally compute the true voting data: $X_{\mathcal{P}} = \widehat{M}^{-1} E(Y_{\mathcal{P}})$. However, since the theoretical expectation $E[Y_{\mathcal{P}}]$ is unobservable in reality, we cannot solve for the absolutely true $X_{\mathcal{P}}$. In actual calculations, we must replace the unknowable $E[Y_{\mathcal{P}}]$ with the actual observed vector $Y_{\mathcal{P}}$. Finally we can derive an estimator of the true value: $\widehat{X}_{\mathcal{P}} = \widehat{M}^{-1} Y_{\mathcal{P}}$.

Variance of the Observed Voting Data Y

In last Section 5.3, we get the estimator $\widehat{X} = [\hat{x}_1, ..., \hat{x}_n, \hat{x}_B, \hat{x}_I]$. Now we can update the transition matrix $T(X)$ as a estimator of transition matrix $\widehat{T}$ (with the estimator of weight $\hat{w}_j$):

$$\widehat{T} = \left[\begin{array}{cccccc|cc} 1-\epsilon & \epsilon_{\mathcal{P}} p_2 & 0 & \dots & 0 & 0 & \zeta_{\mathcal{P}} \hat{w}_1 & \eta_{\mathcal{P}} \hat{w}_1 \\ \epsilon_{\mathcal{P}} & 1-\epsilon & \epsilon_{\mathcal{P}} p_3 & \dots & 0 & 0 & \zeta_{\mathcal{P}} \hat{w}_2 & \eta_{\mathcal{P}} \hat{w}_2 \\ 0 & \epsilon_{\mathcal{P}}(1-p_2) & 1-\epsilon & \dots & 0 & 0 & \zeta_{\mathcal{P}} \hat{w}_3 & \eta_{\mathcal{P}} \hat{w}_3 \\ \vdots & \vdots & \vdots & \ddots & \vdots & \vdots & \vdots & \vdots \\ 0 & 0 & 0 & \dots & 1-\epsilon & \epsilon_{\mathcal{P}} & \zeta_{\mathcal{P}} \hat{w}_{n-1} & \eta_{\mathcal{P}} \hat{w}_{n-1} \\ 0 & 0 & 0 & \dots & \epsilon_{\mathcal{P}}(1-p_{n-1}) & 1-\epsilon & \zeta_{\mathcal{P}} \hat{w}_n & \eta_{\mathcal{P}} \hat{w}_n \\ \hline \epsilon_B & \epsilon_B & \epsilon_B & \dots & \epsilon_B & \epsilon_B & 1-\zeta & \eta_B \\ \epsilon_I & \epsilon_I & \epsilon_I & \dots & \epsilon_I & \epsilon_I & \zeta_I & 1-\eta \end{array}\right]$$

According to the variance formula of the binomial distribution, our counting error model (see Section 5.1), and the distribution of $\mathbf{V^{(j)}}$, $\mathbf{V^{(B)}}$ and $\mathbf{V^{(I)}}$ (see Section 5.2). We can formulate the variance of parties' events with boundary condition $x_0 = x_{n+1} = 0$, $p_1 = 0$, and $p_n = 1$.

$$\text{Var}(y_j) = \text{Var}(V_{j-1\to j}) + \text{Var}(V_{j\to j}) + \text{Var}(V_{j+1\to j}) + \text{Var}(V_{B\to j}) + \text{Var}(V_{I\to j})$$

Since the misclassification events originating from different vote sources are independent, the variance of the observed sum is exactly the sum of their individual variances. Applying the binomial variance formula $Var = np(1-p)$ to each mutually exclusive path yields:

$$\begin{aligned} \text{Var}(V_{j-1\to j}) &= x_{j-1} \cdot \epsilon_{\mathcal{P}}(1-p_{j-1}) \cdot [1-\epsilon_{\mathcal{P}}(1-p_{j-1})] \\ \text{Var}(V_{j\to j}) &= x_j \cdot (1-\epsilon) \cdot \epsilon \\ \text{Var}(V_{j+1\to j}) &= x_{j+1} \cdot \epsilon_{\mathcal{P}} p_{j+1} \cdot (1-\epsilon_{\mathcal{P}} p_{j+1}) \\ \text{Var}(V_{B\to j}) &= x_B \cdot (\zeta_{\mathcal{P}} w_j) \cdot (1-\zeta_{\mathcal{P}} w_j) \\ \text{Var}(V_{I\to j}) &= x_I \cdot (\eta_{\mathcal{P}} w_j) \cdot (1-\eta_{\mathcal{P}} w_j) \end{aligned}$$

Hence the estimator of variance of party j is given by:

$$\widehat{\text{Var}}(y_j) = \sum_{k=1}^{n+2} x_k \cdot \widehat{T}_{j,k}(1-\widehat{T}_{j,k}) \tag{8}$$

By applying this decomposition logic across blank and invalid parts.

$$\widehat{\text{Var}}(y_B) = \sum_{k=1}^{n+2} x_k \cdot \widehat{T}_{n+1,k}(1-\widehat{T}_{n+1,k}) \tag{9}$$

$$\widehat{\text{Var}}(y_I) = \sum_{k=1}^{n+2} x_k \cdot \widehat{T}_{n+2,k}(1-\widehat{T}_{n+2,k}) \tag{10}$$

Estimated Covariance of the Observed Voting Data Y

Define the estimator of covariance matrix of Y as $\hat{\Sigma}_Y$ and set $i = \{1, 2, \ldots, n, B, I\}$:

$$\widehat{\Sigma}_Y = \left[\begin{array}{cccccc|cc} V_1 & C_{1,2} & C_{1,3} & \ldots & \ldots & C_{1,n} & C_{1,B} & C_{1,I} \\ C_{2,1} & V_2 & C_{2,3} & \ldots & \ldots & C_{2,n} & C_{2,B} & C_{2,I} \\ C_{3,1} & C_{3,2} & V_3 & \ldots & \ldots & C_{3,n} & C_{3,B} & C_{3,I} \\ \vdots & \vdots & \vdots & \ddots & & \vdots & \vdots & \vdots \\ \vdots & \vdots & \vdots & & \ddots & \vdots & \vdots & \vdots \\ C_{n,1} & C_{n,2} & C_{n,3} & \ldots & \ldots & V_n & C_{n,B} & C_{n,I} \\ \hline C_{B,1} & C_{B,2} & C_{B,3} & \ldots & \ldots & C_{B,n} & V_B & C_{B,I} \\ C_{I,1} & C_{I,2} & C_{I,3} & \ldots & \ldots & C_{I,n} & C_{I,B} & V_I \end{array}\right]$$

Based on the properties of the multinomial distribution, we consider the covariance between two different outcomes $i, m \in \{1, \ldots, n, B, I\}$, originating from the same initial vote source $k \in \{1, \ldots, n, B, I\}$:

$$\text{Cov}(V_{k\to i}, V_{k\to m}) = -x_k \cdot \widehat{T}_{i,k} \cdot \widehat{T}_{m,k} \quad \text{(when } i \neq m\text{)}$$

Errors from different vote sources are independent. How vote source k is distributed has no impact on how vote source l is distributed. Therefore, when $k \neq l$, for any targets $i, m \in \{1, \ldots, n, B, INV\}$:

$$\text{Cov}(V_{k\to i}, V_{l\to m}) = 0$$

Hence the elements of covariance matrix Σ_Y are:

$$V_i = \widehat{\text{Var}}(y_i), \quad \text{(equal to Equation 8,9,10, when } i = m\text{)}$$

$$C_{i,m} = -\sum_{k=1}^{n+2} x_k \cdot \widehat{T}_{i,k} \cdot \widehat{T}_{m,k}, \quad \text{(when } i \neq m\text{)}$$

Derivation of Variance of $\widehat{X}$

The covariance matrix of a random vector $\widehat{X}$ is defined, and

$$\widehat{\Sigma}_{\widehat{X}} = \text{Cov}(\widehat{X}, \widehat{X}) = E\left[(\widehat{X} - E[\widehat{X}])(\widehat{X} - E[\widehat{X}])^T\right]$$

Since $\widehat{T}^{-1}$ is treated as a constant matrix, we can move the expectation operator inside the linear transformation due to the linearity of expectation: $E[\widehat{X}] = E[\widehat{T}^{-1}Y] = \widehat{T}^{-1}E[Y]$.

$$\widehat{\Sigma}_{\widehat{X}} = \widehat{T}^{-1}\widehat{\Sigma}_Y(\widehat{T}^{-1})^T$$

Hence we can derive the variance from the diagonal elements of Σ_X:

$$(\widehat{\Sigma}_{\widehat{X}})_{i,i} = \text{Var}(\widehat{X})$$

Confidence Intervals for True Vote

Finally we approximate the distribution with $\widehat{X} \sim \mathcal{N}(E(\widehat{X}), \text{Var}(\widehat{X}))$, and:

$$E[\widehat{X}] = E[\widehat{T}^{-1}Y] = \widehat{T}^{-1}E[Y] = \widehat{T}^{-1}(\widehat{T}X) = X$$

Let $\hat{\sigma}_i = \sqrt{(\widehat{\Sigma}_{\widehat{X}})_{i,i}}$ be the estimated standard deviation of $\hat{x}_i$. According to the standard normal distribution table, the 95% confidence intervals are approximated by:

$$P(-1.96 \leq \frac{\hat{x}_i - x_i}{\hat{\sigma}_i} \leq 1.96) \approx 0.95$$

$$P(\hat{x}_i - 1.96\hat{\sigma}_i \leq x_i \leq \hat{x}_i + 1.96\hat{\sigma}_i) \approx 0.95$$

Hence we can finally derive the true voting data interval:

$$x_i \in [\hat{x}_i - 1.96\hat{\sigma}_i, \quad \hat{x}_i + 1.96\hat{\sigma}_i]$$

5.4 Model and Parameter Setup

This section uses official ballot data[26] as the observation data $X_{\mathcal{P}} = [x_1, x_2, \ldots, x_n]^T$ for the model. Since the official party ranking is based on the number of votes received from largest to smallest[26], we re-ranked the official ballot data based on the horizontal party ranking on actual ballot paper[16]. Finally, we implemented the counting error model (see Section 5.1) by using the numerical simulation calculations and visualization via Python.

Based on the Dutch TK ballot paper (see Figure 4), we assume that the visual offset during manual vote counting is symmetrical. Therefore, the probability of a ballot being misclassified to the left or right of an adjacent party is equal, i.e., $p_j = 0.5$ (where $1 < j < n$). Misclassification of ballots to border parties can only occur in one direction.

The final total counting discrepancy was 7,766 votes, corresponding to 72.99 discrepancies per 100,000 cast votes[17]. With 10,571,990 valid candidate votes, this gives

$$\epsilon = \frac{7766}{10571990} \approx 0.0007346$$

Since no official dataset directly reports the direction of each misclassified ballot, the other transition parameters are set by the following assumption:

- Most of this error is assigned to valid-party-to-valid-party misclassification, because the largest detected counting-error category in the is the swapping of candidate votes. Hence we set:

$$\epsilon_{\mathcal{P}} = 0.95\epsilon$$

- The probability of a valid ballot being misjudged as blank or invalid should be very low. Invalid ballots usually involves multiple markings, incorrect markings, or non-compliant entries. However, a blank ballot is easily identifiable because it contains no entries. Therefore, the probability of a valid ballot being misjudged as invalid is much higher than that being misjudged as blank. Hence we set:

$$\epsilon_B = 0.8(1 - \epsilon_{\mathcal{P}}), \qquad \epsilon_I = 0.2(1 - \epsilon_{\mathcal{P}}).$$

- Similarly, since blank ballots have no entries, only a very small number are misplaced due to vote counter fatigue or error. Similarly, invalid votes are more likely to be assigned to valid political parties. Hence we set:

$$\zeta = 0.0005, \qquad \zeta_{\mathcal{P}} = 0.8\zeta, \qquad \zeta_I = 0.2\zeta,$$

$$\eta = 0.005, \qquad \eta_{\mathcal{P}} = 0.8\zeta, \qquad \eta_I = 0.2\zeta.$$

5.5 Result

5.5.1 Impact on Real (error-free) Vote Distribution

Figure 5 shows the difference between the observed vote counts and the estimated real error-free vote counts under the counting error model. The horizontal axis represents the vote correction, defined as

$$\Delta_i = \hat{x}_i - y_i,$$

A positive correction ($\Delta_i > 0$, meaning $\hat{x}_i > y_i$) indicates that the model estimates a specific party's real vote count to be higher than its observed count. Conversely, a negative correction ($\Delta_i < 0$, meaning $\hat{x}_i < y_i$) indicates that the estimated real vote count is lower than the observed count. The vertical axis lists all parties on the ballot paper's order, together with the blank and invalid ballot categories. The length of the bar shows the magnitude of the correction. The numerical labels at the end of the bars report the estimated values of Δ_i. In addition, the black error bars represent the corresponding 95% confidence intervals.

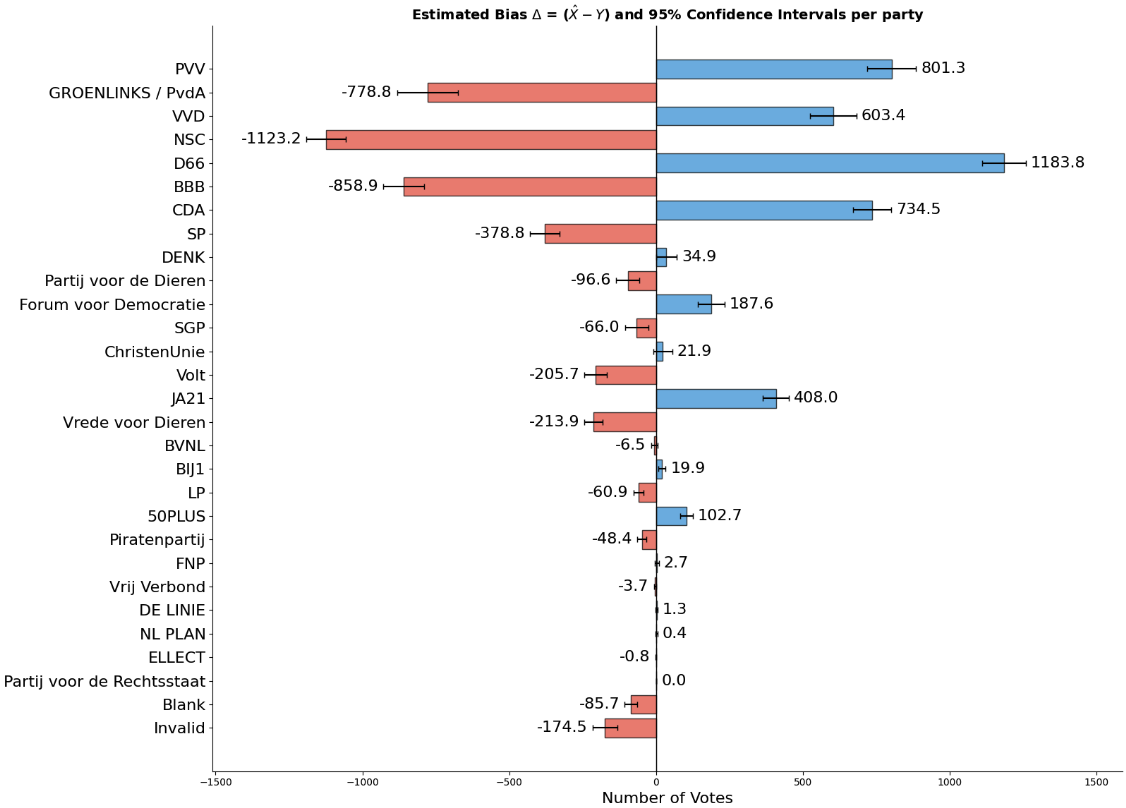

FIGURE 5: Estimated bias $\Delta = (\hat{X} - Y)$ and 95% confidence intervals per party.

The bar plot The quantitative results from the bar chart show an asymmetric distribution. First, major parties with large foundational vote counts (such as D66, PVV, and CDA) exhibit positive biases, indicating a reduction in their votes during the counting process (losing an estimated 1183.8, 801.3, and 734.5 true votes, respectively). These parties have large vote bases, which generate a high volume of spatial misclassification, while their adjacent parties have relatively smaller vote volumes.

NSC is the most extreme negative bias ($\Delta = -1123.2$). Because it is physically positioned adjacent to VVD and D66, NSC received spatial errors originating from these two large adjacent parties, causing the official statistics to overestimate its true vote share. BBB ($\Delta = -858.9$), positioned adjacent to D66 and CDA, shows a negative bias driven by the same physical mechanism.

Furthermore, as PVV is positioned at the border of the ballot paper, its spatial misallocation can only transfer in one direction, resulting in a net reduction in votes. The micro-parties at the tail of the ballot (such as FNP, DE LINIE, etc.) have low vote bases, as do their local neighbors. Consequently, the spatial errors they generate tend to approach zero, leaving them largely unaffected spatial misclassification.

Finally, the invalid ($\Delta = -174.5$) and blank ($\Delta = -85.7$) categories both show negative biases. This indicates that misclassifications related to blank and invalid votes are not a major source of the overall discrepancy.

The 95% confidence interval For all political parties that were affected (such as D66, NSC, and PVV), their confidence intervals did not intersect the zero axis. Overall, the confidence intervals for the major parties are relatively narrow compared with the magnitude of their estimated corrections. We can confidently determine whether these parties experienced a net loss or net gain in votes. For example, D66, PVV, CDA, and VVD have positive corrections, with their 95% confidence intervals mainly located on the positive side of zero.

For some political parties, such as CU, although the point estimate correction is positive, their 95% confidence interval crosses zero. For several smaller parties (FNP, DE LINIE etc.), the estimated corrections are close to zero, and their 95% confidence intervals are relatively large compared with the correction values themselves. This implies that it is statistically indeterminate whether these parties finally gained or lost votes due to counting errors. The corrections for blank and invalid ballots are also small, indicating that the uncertainty related to blank and invalid ballots does not change the overall party vote distribution.

The counting error model has an effect on the estimated real vote counts, but it does not indicate a large-scale deviation from the official vote distribution.

5.5.2 Sensitivity Analysis on Seat Allocation

To analyze the system's sensitivity, we varied the primary error ϵ (the valid vote misclassification rate) by simulating $\{0, 500, \ldots, 1000000\}$ error votes with steps of 500. All other parameters remain consistent with Section 5.4. For each misclassification rate, we calculated the estimator of real votes $\hat{X}$ and applied the D'Hondt method to allocate seats. The results were then compared with the baseline (TK25) to record the changes, as presented in the table 3.

The sensitivity analysis shows robust outcomes, as summarized in Table 3 (note that 'init' in the table denotes initial seats). Within the range of 0 to 9,000 misclassified votes, the seat distribution remains unchanged. With the current 7,766 misclassified votes, there will be no impact on the changes in seating arrangements. The system reaches the first tipping point at 10,000 misclassified votes. A single seat transfer occurs: the small party SP loses one slack, which transferred to large party D66.

As the error votes raised to $11,000$ and $113,500$, the final inter-party seat transfer remains at SP to D66. The growing error merely triggers internal composition flips between initial and remainder seats (internal swaps) for larger party PVV and medium party JA21.

Table 3: Sensitivity analysis of seat allocation under different error votes.

Error Votes	$\epsilon\%$	Seat Changes	Losing Seats	Gaining Seats	Internal Swaps
...	...	...	...	...	...
10,000	0.0946%	1	SP $\downarrow$ 1 (slack)	D66 $\uparrow$ 1 (slack)	None
11,000	0.1040%	2	SP $\downarrow$ 1 (slack)	D66 $\uparrow$ 1 (slack)	PVV: init $\uparrow$ 1, slack $\downarrow$ 1
...	...	...	...	...	...
113,500	1.0736%	3	SP $\downarrow$ 1 (slack)	D66 $\uparrow$ 1 (slack)	PVV: init $\uparrow$ 1, slack $\downarrow$ 1, JA21: init $\uparrow$ 1, slack $\downarrow$ 1
...	...	...	...	...	...

6 Voter Uncertainty Model

Dutch voters are mobile, but they don't vote randomly[2]. They are typically loyal to a political alliance, but no longer loyal to a particular party[2]. In the Netherlands, the terms "left" and "right" are commonly used to classify parties, "progressive" and "conservative" are also used to supplement the classification[20]. However, this classification is often controversial, there is a relatively vague gray area in the political center[20].

We divided 27 parties into 5 political blocs based on the potential shift in voters and the political ideology of parties[16][20][4]. The classification Table 4 and rationale for the five voter-transition blocs are shown as follows:

Table 4: Electoral results and classifications by voter-transition blocs.

Bloc	Name	Parties	Total Votes	Vote Share	Seats
$\mathcal{B}_1$	Left-social and redistributive bloc	GL-PvdA, SP, BIJ1, DENK	1,842,476	17.43%	26
$\mathcal{B}_2$	Green-progressive and progressive-liberal bloc	D66, Volt, PvdD, Piratenpartij, Vrede voor Dieren, ELLECT, Partij voor de Rechtsstaat	2,154,223	20.38%	30
$\mathcal{B}_3$	Centrist, Christian-democratic and governance bloc	CDA, NSC, CU, SGP, 50PLUS, FNP, NL PLAN	1,888,419	17.86%	26
$\mathcal{B}_4$	Market-liberal and centre-right bloc	VVD, LP, Vrij Verbond	1,515,125	14.33%	22
$\mathcal{B}_5$	Conservative, right-populist and nationalist bloc	PVV, JA21, FvD, BBB, BVNL, DE LINIE	3,171,747	30.00%	46

$\mathcal{B}_1$ (Left-social and redistributive bloc): GL-PvdA and SP belong to the left-wing/social democratic space. BIJ1 is radical left, DENK is usually counted in the left-wing camp.

$\mathcal{B}_2$ (Green-progressive and progressive-liberal bloc): D66 and Volt represent the progressive-liberal centre-left space, while PvdD, Vrede voor Dieren and the Piratenpartij are issue-based parties with strong ecological, animal-rights or civil-liberty profiles. ELLECT and Partij voor de Rechtsstaat are included here as small reform-oriented parties.

$\mathcal{B}_3$ (Centrist, Christian-democratic and governance bloc): CDA is a Christian democratic centrist party. CU and SGP are confessional parties. NSC's position is harder to define but leans towards governance/centrist. 50PLUS, FNP, and NL PLAN are more like interest/regional/representative parties, so placing them in the centrist governance bloc as a residual centrist group. FNP primarily represents Frisian language/culture, and NL PLAN emphasizes giving Asian-Dutch individuals a political voice.

$\mathcal{B}_4$ (Market-liberal and centre-right bloc): VVD is right-liberal/market-liberal. LP explicitly advocates for maximum individual freedom and minimal government, making it suitable for the market-liberal bloc.

$\mathcal{B}_5$ (Conservative, right-populist and nationalist bloc): PVV, JA21 and FvD belong to the right-wing/right-populist space. BBB is a rural/agricultural conservative populist type. BVNL is described as conservative-liberal and populist. DE LINIE emphasizes security, immigration control, and livelihood security, making it more reasonable to place it in the conservative right-wing bloc.

Ideological similarity The five voter-transition blocs ($\mathcal{B}_1$ to $\mathcal{B}_5$) constitute a continuous ideological spectrum, ans we assume that it follows to the spatial voting "Neighbor Model" in Section 5.1. Adjacent blocs exhibit policy overlap, facilitating stepwise voter mobility.

Specifically, $\mathcal{B}_1$ and $\mathcal{B}_2$ converge on egalitarian issues, while $\mathcal{B}_2$ and $\mathcal{B}_3$ connect through moderate institutionalism. Further along the spectrum, $\mathcal{B}_3$ and $\mathcal{B}_4$ align via economic pragmatism, and finally, $\mathcal{B}_4$ and $\mathcal{B}_5$ bridge over tightening national sovereignty and immigration controls.

6.1 Potential Voter Transfer Model

This section models voter uncertainty as a stochastic vote-transfer process. In contrast to the counting error model, voter uncertainty refers to possible changes in voters' final party choices before casting their ballots. Define $i, j \in \{1, \ldots, 27\}$ be the index of party, $k \in \{1, ..., 5\}$ be the index of bloc. Recall that the observed vote vector of TK25 is denoted by: $Y_{\mathcal{P}} = [y_1, y_2, ..., y_n]^T$. The aim of this model is to construct a perturbed vote vector: $Z_{\mathcal{P}} = [z_1, z_2, ..., z_n]^T$, which is given by:

$$Z_{\mathcal{P}} = Y_{\mathcal{P}} \cdot A$$

where A is the potential voter transfer matrix. And for each bloc k, four parameters are introduced: $\alpha_k \in [0, 1]$ represents the proportion of voters in bloc k who are uncertain, $\beta_k \in [0, 1]$ is the proportion of uncertain voters from bloc k who move to a different bloc, $p_k \in [0, 1]$ and $1 - p_k \in [0, 1]$ represent the probabilities of moving to the left bloc $(k - 1)$ and the right bloc $(k + 1)$, respectively, and $\omega_{i,k} \in [0, 1]$ denotes the weight of party i in bloc k.

Therefore, for voters originally supporting a party in bloc k, the probabilities of the three possible outcomes are defined as follows: they remain with the original party with probability $1 - \alpha_k$, switch to another party within the same bloc with probability $\alpha_k(1 - \beta_k)$, or switch to a party in a different bloc, moving to the left with probability $p_k \alpha_k \beta_k$, and to the right with probability $(1 - p_k)\alpha_k \beta_k$.

When voters switch to another party j within the same bloc, we assume they choose the target party proportionally to its weight among the remaining parties, which is defined by the normalized factor $\frac{\omega_{j,k}}{1-\omega_{i,k}}$. Let A be the 27×27 transition matrix, where A_{ij} denotes the probability that a voter originally supporting party i finally votes for party j. The transition probability is defined by:

$$A_{ij} = \begin{cases} 1 - \alpha_k & \text{if } i = j \text{ and } i, j \in \mathcal{B}_k \\ \alpha_k(1 - \beta_k) \cdot \frac{\omega_{j,k}}{1-\omega_{i,k}} & \text{if } i \neq j \text{ and } i, j \in \mathcal{B}_k \\ p_k \alpha_k \beta_k \cdot \omega_{j,k-1} & \text{if } i \neq j \text{ and } i \in \mathcal{B}_k,\ j \in \mathcal{B}_{k-1} \\ (1 - p_k)\alpha_k \beta_k \cdot \omega_{j,k+1} & \text{if } i \neq j \text{ and } i \in \mathcal{B}_k,\ j \in \mathcal{B}_{k+1} \end{cases}$$

6.2 Monte Carlo Simulation

To capture the stochastic nature of vote transfers, we assume the realized voter flows follow a multinomial distribution. For each party $i \in \{1, \ldots, 27\}$, let $Z_i = (Z_{i,1}, Z_{i,2}, \ldots, Z_{i,27})$ be a random vector, where $Z_{i,j}$ represents the number of voters originally supporting party i who finally cast their ballots for party j.

Given the original vote count y_i and the row $A_{i,\cdot}$ of our proposed transition matrix A. The destinations of the y_i votes are sampled from a multinomial distribution:

$$Z_i \sim \text{Multinomial}(y_i, A_{i,1}, A_{i,2}, \ldots, A_{i,27})$$

To quantify the impact of voter uncertainty on election results, we employ Monte Carlo simulation to generate R possible final vote distributions. In each simulation, we generate the perturbation voting vector $Z'^{(r)}$ for that simulation by summing the columns of all sampled flow direction matrices:

$$Z'^{(r)} = \{z'^{(r)}_1, ..., z'^{(r)}_{27}\}, \quad z'^{(r)}_j = \sum_{i=1}^{27} Z_{i,j}$$

The above sampling process is repeated R times to construct a set of R possible final voting vectors: $\mathcal{Z}' = \{Z'^{(1)}, \ldots, Z'^{(R)}\}$

6.3 Model and Parameter Setup

We used the official TK25 election data and categorized the participating parties into their respective political blocs. Within each bloc, we arranged the parties in descending order of their official vote counts. Finally, we applied the voter uncertainty model to this rearranged dataset, implementing a Monte Carlo simulation with $R = 100,000$ iterations. The assumed uncertainty and transition parameters for all five political blocs are summarized in Table 5. The rationale for these specific parameter choices is detailed below.

TABLE 5: Assumed transition parameters for the voter uncertainty model by political bloc.

Bloc (k)	α_k	β_k	p_k
$\mathcal{B}_1$	0.20	0.30	0
$\mathcal{B}_2$	0.35	0.45	0.60
$\mathcal{B}_3$	0.40	0.30	0.50
$\mathcal{B}_4$	0.25	0.40	0.30
$\mathcal{B}_5$	0.15	0.10	1

In TK25, 40% of voters make their choice in the last few days before the election or on election day, and D66 performs well among late deciders[13]. Therefore, α_k for $\mathcal{B}_2$ and $\mathcal{B}_3$ should be higher than the more stable bloc, and we assume that $\alpha_k \leq 0.4$. Specifically, we set $\alpha_1 = 0.20$, as strong ideological identification results in a relatively stable base, and the merger of GL-PvdA further consolidated left-wing votes, leading to a lower attrition rate. For the second bloc, we assign $\alpha_2 = 0.35$ because this bloc includes mobile parties such as D66, Volt, and PvdD, with D66 playing a bridging role in 2025 and performing well among late deciders[13]. We allocate the highest uncertainty, $\alpha_3 = 0.40$, to the third bloc, since the collapse of NSC and the rise of CDA are both concentrated in this area. Furthermore, we set $\alpha_4 = 0.25$, although VVD has a stable market liberal core, it faces competition from CDA, D66, and JA21[4]. Finally, $\alpha_5 = 0.15$ is assigned because this bloc exhibits clear internal party shifts. For example, the loss in PVV is partially offset by the growth in JA21 and FvD[4].

Voters typically only seriously consider a few parties, and these parties are usually ideologically similar[13]. This suggests that cross-bloc shifts should not be too large, so we assume that $\beta_k \leq 0.5$. Specifically, we set $\beta_1 = 0.30$ and $p_1 = 0$, as high internal integration on the left means uncertain voters mostly switch between GL-PvdA and SP, with the main external outlet being $\mathcal{B}_2$, especially due to the overlap between GL-PvdA/D66/PvdD/Volt. For the second bloc, we assign $\beta_2 = 0.45$ and $p_2 = 0.6$, containing Volt and D66, voters in this bloc flow internally but are also prone to cross into $\mathcal{B}_1$ or $\mathcal{B}_3$, since D66 bridges more robustly towards the left than the right[13]. Furthermore, we establish $\beta_3 = 0.30$ and $p_3 = 0.50$ because $\mathcal{B}_3$ internally includes CDA, NSC, CU, SGP, 50PLUS, etc., demonstrating strong internal redistribution capabilities where uncertain voters are likely to flow leftward to $\mathcal{B}_2$ or rightward to $\mathcal{B}_4$. In addition, we set $\beta_4 = 0.40$ and $p_4 = 0.30$, because VVD often appears in the choice set along with JA21, BBB, and PVV, undecided voters in $\mathcal{B}_4$ are more likely to move towards $\mathcal{B}_5$. Finally, $\beta_5 = 0.10$ and $p_5 = 1$ are assigned because this bloc is one of the most coherent blocs, meaning that most of the switchers in $\mathcal{B}_5$ are transferred within itself.

6.4 Result

6.4.1 Bloc Perspective Voter Uncertainty Transfer Analysis

In Figure 6, the left-social bloc ($\mathcal{B}_1$) experiences an increase of $+143,172.8$ votes. This gain is primarily driven by the coordination within the progressive spectrum.

In contrast, the green-progressive and progressive-liberal bloc ($\mathcal{B}_2$) encounters a notable net loss of $-125,896.1$ votes. Driven by high internal volatility, these voters largely shifted leftward to consolidate support, making $\mathcal{B}_2$ a net donor of votes under systemic uncertainty.

The centrist and governance bloc ($\mathcal{B}_3$) emerges as the primary casualty of electoral volatility, suffering a massive net decrease of $-339,884.6$ votes, severely weakens the parties

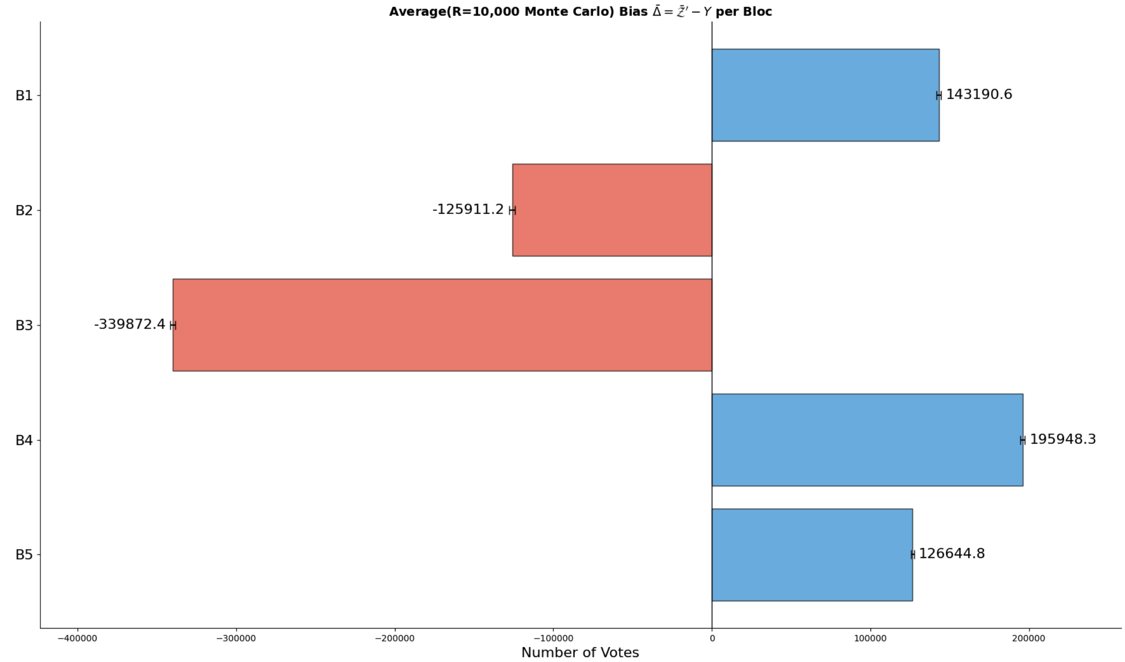

FIGURE 6: Average bias with R=10,000 Monte Carlo per bloc

in the bloc.

Conversely, the market-liberal bloc ($\mathcal{B}_4$) acts as the largest net beneficiary, securing a major influx of $+195,982.2$ votes. It successfully retains its core base while simultaneously absorbing right-leaning defectors from the collapsing center.

Finally, the conservative right bloc ($\mathcal{B}_5$) captures a robust and stable net gain of $+126,625.8$ votes, protected by its intense core voter loyalty.

6.4.2 Party Perspective Voter Uncertainty Transfer Analysis

In Figure 7, within the left-social bloc ($\mathcal{B}_1$), the major party GL-PvdA loses -19,740.3 votes, while more ideologically distinct parties absorb the remaining support, leading to net gains for DENK (+82,312.0), SP (+66,573.3), and BIJ1 (+13,989.5).

The green-progressive bloc ($\mathcal{B}_2$) is characterized by a major collapse of D66, which drops by -347,772.0 votes. These votes subsequently flow into the Partij voor de Dieren (+132,932.9) and Volt (+71,671.8).

In the centrist and governance bloc ($\mathcal{B}_3$), the traditional power CDA suffers the largest single-party lost in the entire simulation, losing -353,628.6 votes. Lacking a rigid ideological anchor, its fluid voter base largely leaves the bloc, while the remaining minor centrist parties experience almost no changes.

Within the market-liberal bloc ($\mathcal{B}_4$), the leading VVD experiences a decline of -9,352.9 votes. In contrast, the libertarian alternative LP gains +182,145.8 votes.

Similarly, within the conservative right bloc ($\mathcal{B}_5$), the dominant PVV loses -39,901.0 votes. These votes are redistributed to smaller parties, yielding net growths for JA21 (+69,413.6), Forum voor Democratie (+57,450.5), and BBB (+36,534.2).

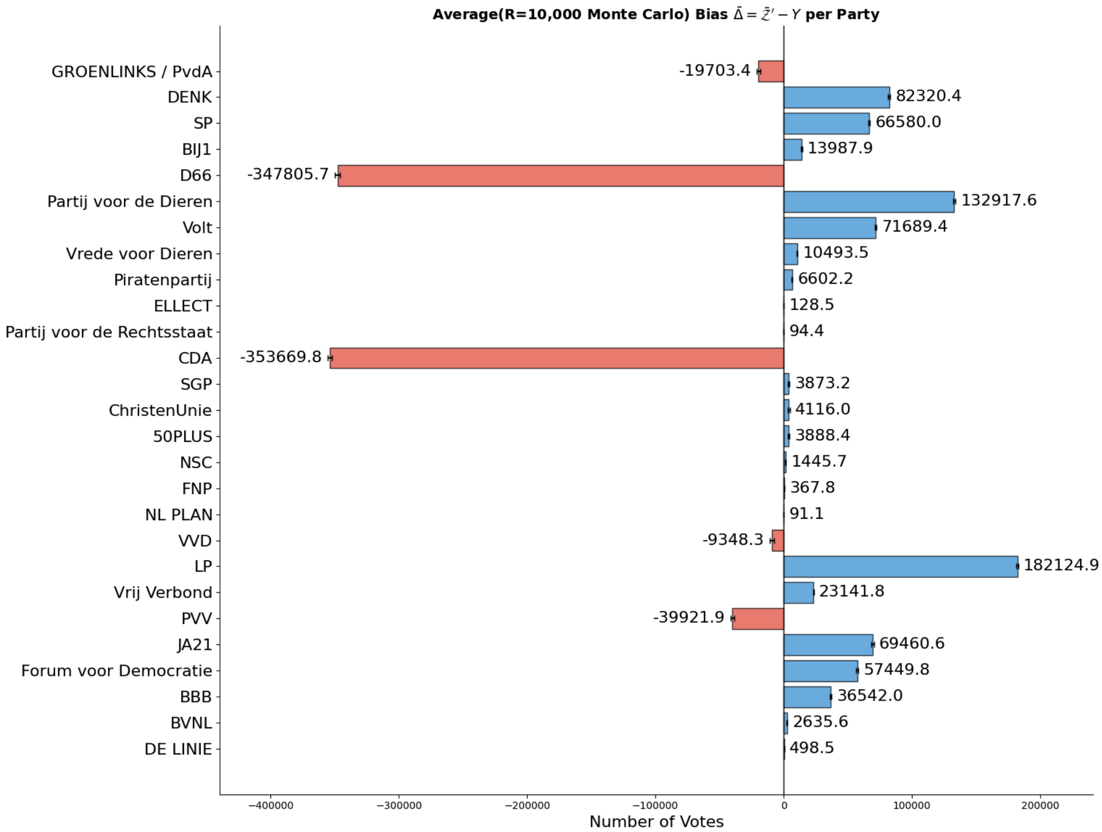

FIGURE 7: Average bias with R=10,000 Monte Carlo per party

7 Public Opinion Research

Based on the party classification in Section 6, we focus on the 16 major political parties for which polling data from the global market research company *Ipsos I&O*[14]. This dataset records the polling voter share data for 16 major political parties from TK23 election to TK25 election. These 16 parties are selected because they account for over 99% of the total vote share in the election, providing a robust representative sample for our analysis. We re-aggregated these parties according to Table 4, including the 15 parties that entered parliament and NSC. As shown in Table 6, the vote share of each bloc remained almost unchanged, and the total number of seats remained constant.

7.1 Voter Shift from TK23 to TK25

Based on the polling data from TK23 to TK25, we explore two questions: how voter uncertainty manifests across different parts of the political spectrum, and how it persists within the same political spectrum. For each political party $i \in \{1, \ldots, 27\}$ and each time point $t \in \{1, \ldots, T\}$, let $V_{i,t}$ denote the vote share of party i in the t-th poll. To evaluate this, we define two indicators.

First, we utilize the standard deviation of the vote share, defined as:

$$\sigma_i^{vote} = \sqrt{\frac{1}{T-1} \sum_{t=1}^{T} (V_{i,t} - \bar{V}_i)^2}$$

where $\bar{V}_i = \frac{1}{T} \sum_{t=1}^{T} V_{i,t}$ is the mean vote share. A larger σ_i^{vote} indicates that the party's

Table 6: Electoral results and classifications by filtered voter transition blocs.

Bloc	Name	Parties	Total Votes	Vote Share	Seats
$\mathcal{B}_1$	Left-social and redistributive bloc	GL-PvdA, SP, DENK	1,802,116	17.23%	26
$\mathcal{B}_2$	Green-progressive and progressive-liberal bloc	D66, Volt, PvdD	2,126,473	20.33%	30
$\mathcal{B}_3$	Centrist, Christian-democratic and governance bloc	CDA, NSC, CU, SGP, 50PLUS	1,876,789	17.94%	26
$\mathcal{B}_4$	Market-liberal and centre-right bloc	VVD	1,505,829	14.39%	22
$\mathcal{B}_5$	Conservative, right-populist and nationalist bloc	PVV, JA21, FvD, BBB	3,149,792	30.11%	46

vote share is more volatile, serving as our primary metric for measuring voter uncertainty.

Second, we consider the range of the vote share, given by:

$$R_i^{vote} = \max_{t \in \{1,\dots,T\}} (V_{i,t}) - \min_{t \in \{1,\dots,T\}} (V_{i,t})$$

where R_i^{vote} represents the difference between the highest and lowest support rates observed for party i across the set of all polls.

7.2 Linear Regression of Polling Errors over Time

To investigate whether the polling accuracy improves as the election approaches, we model the relationship between the temporal distance to the election and the polling error.

Dependent and independent variable. The actual vote share of party i in TK25 is V_i^{TK25}. Then the error for this party in this poll is: $|V_{i,t} - V_i^{TK25}|$. Averaging across all n parties:

$$MAE_t^{vote} = \frac{1}{n} \sum_{i=1}^{n} |V_{i,t} - V_i^{TK25}|.$$

This value is the mean absolute vote share error for the t-th poll. It is the dependent variable, which is the target to be explained in the regression.

The independent variable is d_t, representing the number of days between the t-th poll and the Dutch TK25 election day. For example, if the Dutch TK25 election day is 29 October 2025 and a poll's fieldwork period ends on 28 October 2025, we have $d_t = 29 - 28 = 1$.

Linear regression model. Now we have many pairs of data (d_t, MAE_t^{vote}). The mean vote share error of the t-th poll can be explained by how many days are left until the election. The theoretical linear model is constructed as:

$$MAE_t^{vote} = \beta_0 + \beta_1 d_t + \varepsilon_t$$

where MAE_t^{vote} is the mean polling error for the t-th poll and d_t represents the number of days remaining until the election. In this model, β_0 indicates the theoretical polling error at the time of the election ($d_t = 0$), while β_1 quantifies the average change in error for each additional day away from the election. The term ε_t denotes the random error that the model cannot explain, which we assume follows a normal distribution $\varepsilon_t \sim \mathcal{N}(0, \sigma^2)$.

To estimate these theoretical parameters from the sample data, we employ the Ordinary Least Squares (OLS) method. In this context, the best-fitting line is defined as the line that minimizes the sum of squared vertical distances between the observed polling errors and the values predicted by the linear model. The estimated regression equation is given by:

$$\widehat{MAE}_t^{vote} = \hat{\beta}_0 + \hat{\beta}_1 d_t$$

For each actual data point, the prediction error, also known as the residual, is the difference between the observed and predicted mean absolute error:

$$\hat{\varepsilon}_t = MAE_t^{vote} - \widehat{MAE}_t^{vote} = MAE_t^{vote} - (\hat{\beta}_0 + \hat{\beta}_1 d_t)$$

The OLS approach selects the estimators $\hat{\beta}_0$ and $\hat{\beta}_1$ by minimizing the objective function, which evaluates the sum of these squared residuals:

$$\min_{\beta_0, \beta_1} \sum_{t=1}^{T} (MAE_t^{vote} - \beta_0 - \beta_1 d_t)^2$$

By taking the partial derivatives of this objective function with respect to β_0 and β_1 and setting them to zero, we derive the standard closed-form solutions for the estimators. The slope $\hat{\beta}_1$ and intercept $\hat{\beta}_0$ are calculated as:

$$\hat{\beta}_1 = \frac{\sum_{t=1}^{T} (d_t - \bar{d})(MAE_t^{vote} - \overline{MAE}^{vote})}{\sum_{t=1}^{T} (d_t - \bar{d})^2}$$

$$\hat{\beta}_0 = \overline{MAE}^{vote} - \hat{\beta}_1 \bar{d}$$

where $\bar{d}$ and $\overline{MAE}^{vote}$ represent the sample means of the remaining days and the polling errors, respectively.

7.3 Result

7.3.1 Political Party Performance in Public Opinion

Figure 8 shows the polling vote-share trends of 16 parties from TK23 to TK25. Overall, voter uncertainty is mainly concentrated among a few parties with large fluctuations. PVV increased to more than 30% in early 2024, but then declined continuously and fell to around 17% near TK25. This suggests that its voter support was high but not stable. NSC shows the strongest collapse. It started from a high level after TK23, but declined steadily and almost disappeared before TK25. This makes NSC one of the clearest examples of voter uncertainty.

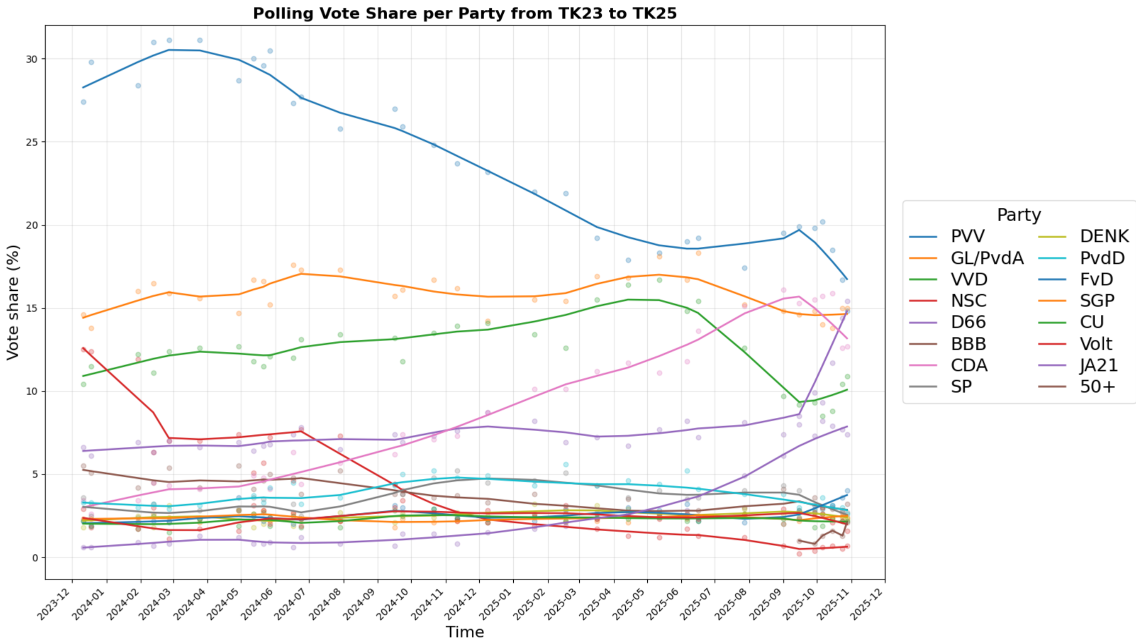

FIGURE 8: Polling vote share per party in opinion polls from TK23 to TK25.

In contrast, D66 and CDan increased clearly in the later period, suggesting that they attracted many floating voters before the election. VVD declined in late 2025, while JA21 increased, which may indicate voter redistribution among right-wing and centre-right parties. GL/PvdA and several smaller parties, such as SGP, CU, PvdD, and DENK, changed only within a smaller range. This indicates a more stable voter base. Therefore, Figure 8 suggests that voter uncertainty is not evenly distributed across all parties, but is mainly concentrated in PVV, NSC, D66, CDA, VVD, and JA21.

Figure 9 quantifies the vote-share volatility of each party from TK23 to TK25. In this context, vote-share volatility is defined as the degree of fluctuation in a party's polling support over time. The bars show the standard deviation of each party's polling vote share, while the shaded area shows the minimum–maximum interval. The results show that PVV has the highest volatility, with a standard deviation of 5.05 percentage points. Its vote share ranges from about 15% to more than 30%, indicating a unstable voter base.

Besides PVV, CDA, NSC, and JA21 also show strong volatility, with standard deviations of 4.50, 3.88, and 2.67, respectively. In particular, NSC has a minimum vote share close to 0%, which confirms its sharp decline during the election cycle. D66 and VVD show medium-level volatility, with standard deviations of 2.58 and 2.09.

In contrast, most smaller parties are relatively stable. For example, SGP, CU, DENK, 50+, and Volt all have standard deviations below 0.60. Overall, Figure 9 shows that voter uncertainty is mainly concentrated in PVV, CDA, NSC, JA21, D66, and VVD, while most smaller parties have a more stable voter base.

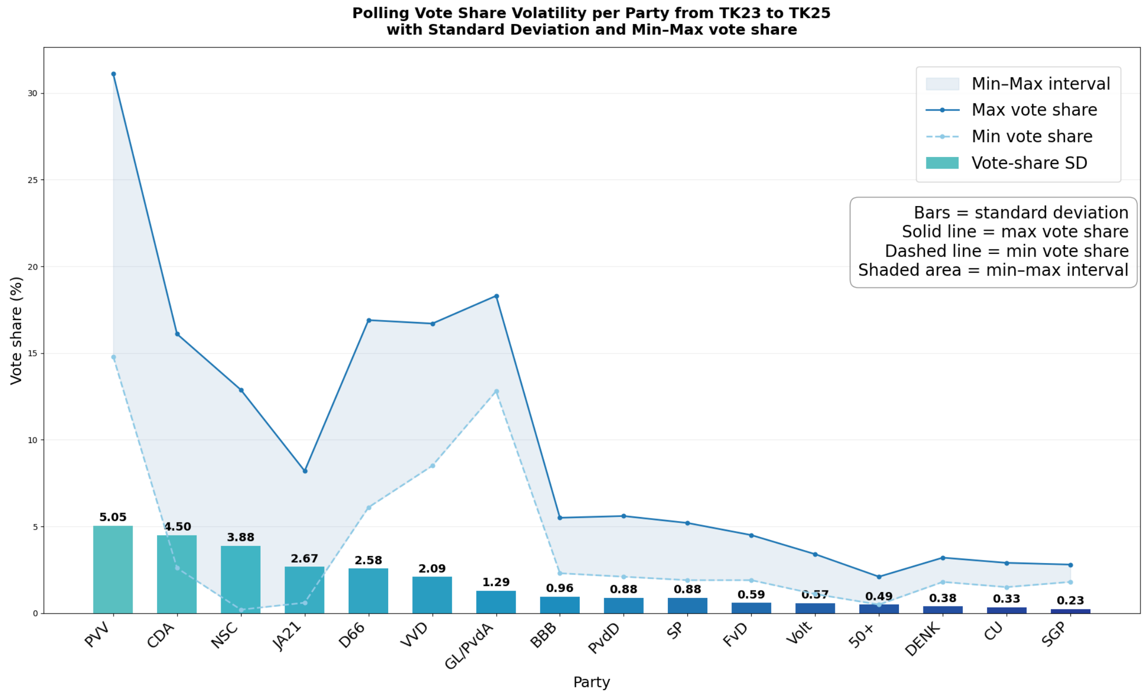

FIGURE 9: Polling vote share volatility per party in opinion polls from TK23 to TK25, with Standard Deviation and Min–Max vote share.

7.3.2 Political Bloc Performance in Public Opinion

As Figure 10 shows, the Conservative, right-populist and nationalist ($\mathcal{B}_5$) bloc consistently maintains the highest overall vote share. Dipping around late 2024 before rebounding as the Dutch TK25 election approaches. A striking voter shift is observable in the Market-liberal and centre-right ($\mathcal{B}_4$) bloc, which suffers a severe and continuous decline in support from mid-2025. Conversely, the Green-progressive and progressive-liberal ($\mathcal{B}_2$) bloc maintains a relatively flat until a upward in the final months preceding the election. Meanwhile, the Centrist, Christian-democratic and governance ($\mathcal{B}_3$) bloc demonstrates a steady, gradual recovery after an early post-TK23 drop. Finally, the Left-social and redistributive ($\mathcal{B}_1$) bloc remains the most visually stable throughout the polling period, peaking slightly mid-term before a gentle decline. These dynamic trends directly shows the high degree of uncertainty and volatility among voters from TK23 to TK25.

TABLE 7: Volatility metrics by political bloc.

Bloc	Party Number	Average SD	Median SD	Max SD
$\mathcal{B}_1$	3	0.850	0.877	1.287 (GL/PvdA)
$\mathcal{B}_2$	3	1.343	0.879	2.577 (D66)
$\mathcal{B}_3$	5	1.887	0.495	4.501 (CDA)
$\mathcal{B}_4$	1	2.093	2.093	2.093 (VVD)
$\mathcal{B}_5$	4	2.318	1.816	5.050 (PVV)
Others	1	0.405	0.405	0.405 (Others)

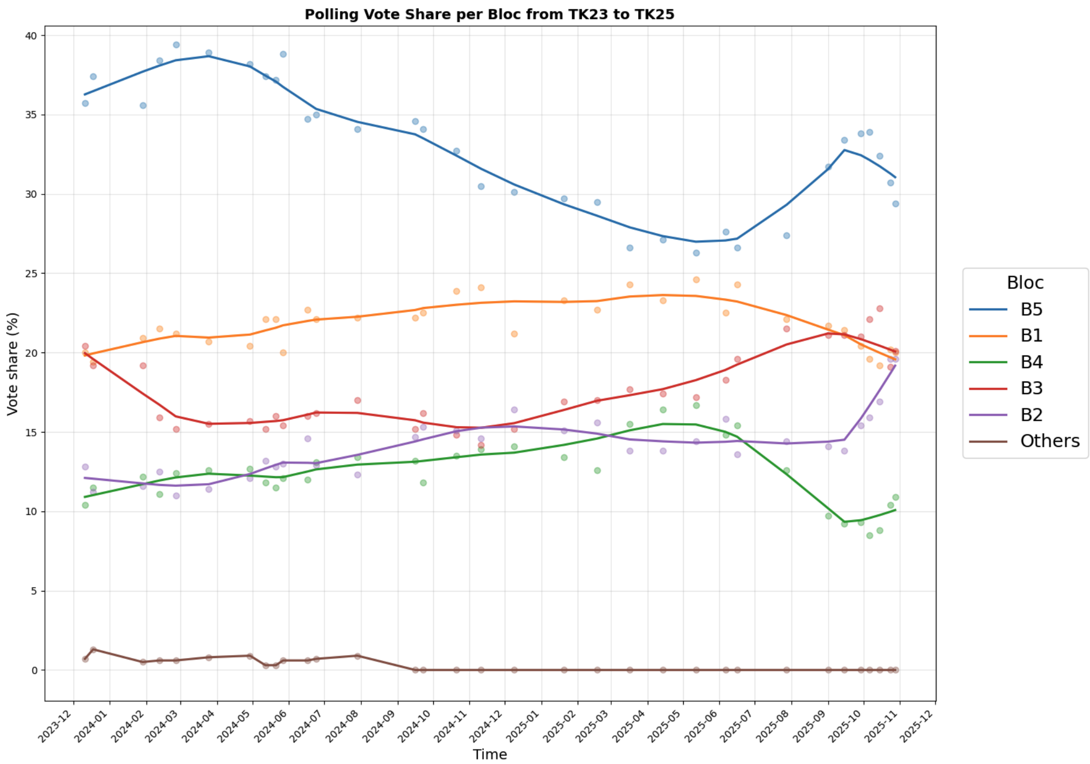

FIGURE 10: Polling vote share per bloc in opinion polls from TK23 to TK25.

Table 7 summarizes the vote-share volatility within each political bloc. The results show that the Conservative, right-populist and nationalist ($\mathcal{B}_5$) bloc has the highest average standard deviation, with 2.318, and its maximum value comes from PVV with 5.050. The Market-liberal and centre-right ($\mathcal{B}_4$) bloc and the Centrist, Christian-democratic and governance ($\mathcal{B}_3$) bloc also show high volatility, with average standard deviations of 2.093 and 1.887, respectively. And the maximum value in the Centrist, Christian-democratic and governance ($\mathcal{B}_3$) bloc comes from CDA with 4.501. In contrast, the Left-social and redistributive ($\mathcal{B}_1$) bloc and Others have lower average standard deviations, with 0.850 and 0.405, respectively. Overall, voter uncertainty is mainly concentrated in the Conservative, right-populist and nationalist ($\mathcal{B}_5$) bloc, the Market-liberal and centre-right ($\mathcal{B}_4$) bloc, and the Centrist, Christian-democratic and governance ($\mathcal{B}_3$) bloc.

7.3.3 Linear Regression Analysis of Polling Errors over Time

Figure 11 shows the relationship between the vote-share mean absolute error and the number of days before the Dutch TK25 election. Each point represents one regular poll. The horizontal axis shows the number of days before election day, denoted by d_t, and the vertical axis shows the vote-share mean absolute error, denoted by MAE_t^{vote}. The estimated regression model is:

$$\widehat{MAE}_t^{vote} = 1.488 + 0.00397 d_t.$$

The intercept is 1.488, represents the predicted vote-share error when $d_t = 0$, that is, theoretically on election day. This value does not have to be zero, because polls may still contain sampling error, pollster effects, and estimation errors.

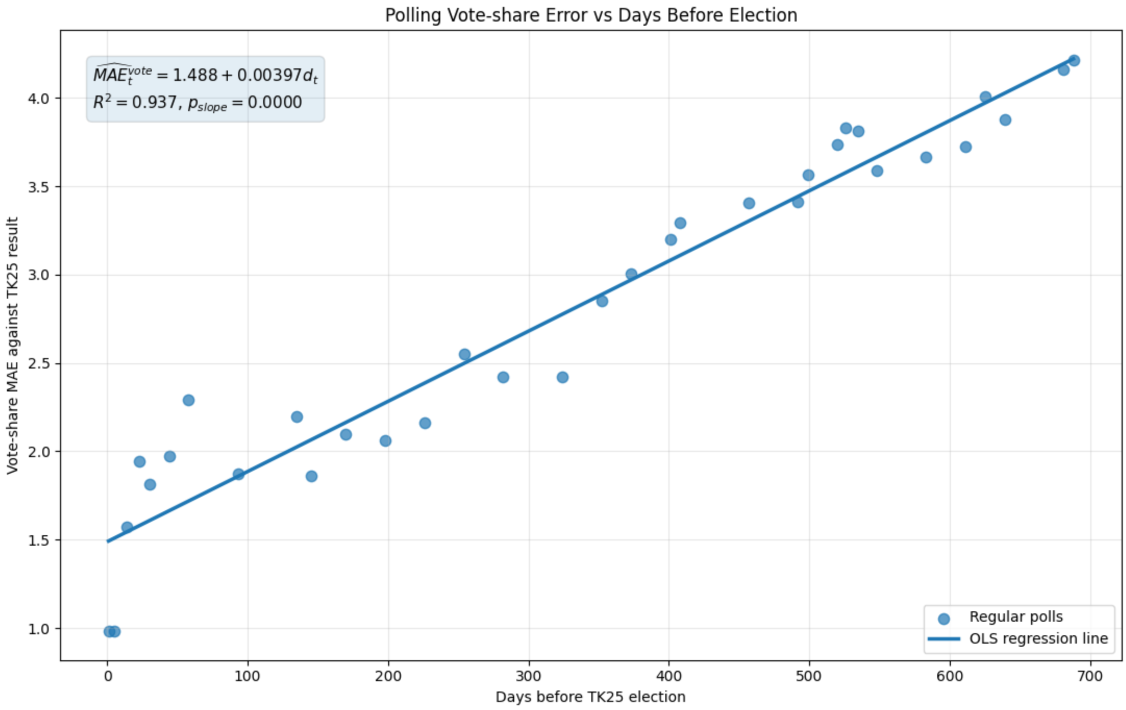

FIGURE 11: MAE-TIME linear regression result

The slope coefficient is 0.00397, measures how much the polling error increases when a poll is conducted one day further away from the election. This means that for every additional 100 days before the election, the predicted vote-share error increases by approximately: $0.00397 \times 100 = 0.397$ percentage points.

Since the slope is positive, polls conducted further away from election day tend to have larger vote-share errors. Equivalently, polls become closer to the final TK25 result as election day approaches. The model has a high explanatory power, with $R^2 = 0.937$. This means that about 93.7% of the variation in vote-share MAE is explained by the number of days before the election.

The p-value of the slope is reported as $p_{\text{slope}} = 0.0000$, which indicates that the positive relationship between days before the election and polling error is statistically significant.

The scatter plot also supports this result. Polls close to election day have relatively low errors, mostly between about 1 and 2 percentage points. In contrast, polls conducted more than 500 days before the election have much larger errors, often between about 3.5 and 4.2 percentage points. The points follow the regression line closely, which is consistent with the high R^2 value.

Therefore, the regression model demonstrates the increasing predictive power of opinion polls as the Dutch TK25 election approached. Earlier polls carry larger forecasting errors, while later polls become more accurate and converge closer to the official TK25 vote-share distribution.

8 Discussion

8.1 The Illusion of Stability under D'Hondt

Given its high dis-proportionality ($LSq = 0.9849$) during all methods in table 2, why does the Netherlands persist with the D'Hondt method? The Dutch 0.67% threshold is low. Lower electoral thresholds will lead to more political parties entering parliament. In this case, adopting a fairer algorithm may lead to a risk of increased fragmentation. Countries need to make choices among different indicators and methods [10]. Raising the constitutional threshold is politically difficult [10]. So in the Dutch House of Commons, D'Hondt method serves as a covert protection, to prevent parliament from fracturing.

However, eliminating micro-parties actually undermines government stability. According to Gamson's Law [11], there is proportionality between the numerical representation of each political force in a government and their number of seats in the parliament. A party's demands (e.g., cabinet positions) scale with its size [11]. For a core coalition holding 74 out of 150 seats, a micro-party with 2 seats is a valuable, low-cost partner.

Using D'Hondt method forces major parties to build majorities with medium or large parties. This increases the friction of negotiations, requiring the surrender of core ministries and compromises [21][8].

8.2 Limitations of Mathematical Models

While the counting error model provides insights in robustness of the seat allocation process, it has two main limitations. First, the spatial misclassification mechanism relies on a physical assumption. In practice, human fatigue or sorting overlaps could cause votes to be misclassified across non-adjacent parties. So the real errors are more random than a neighbor-to-neighbor transfer. Second, the selection of error transition parameters is limited by data availability. Due to the lack of official post-election analysis data, the specific transition probabilities were assigned subjectively based on literature and news. Therefore, post-election analysis data is important for the accuracy of the model.

While the voter uncertainty model shows a high uncertainty in the Dutch TK election, it also has three main limitations. First, classifying all participating parties into five political blocs is relatively subjective. Many small parties or parties focused on a single theme have unclear or overlapping ideologies. Second, the design of the transition matrix cause unexpected outcomes. The present model redistributes cross bloc votes according to how many votes are left for each targeted party but results in small parties receiving an increase in votes, whereas larger parties will experience a decline in their total number of votes. The final issue in this model is its transition parameters due to difficulty in quantifying changes in individual voter's ideologies. Thus we derive these transition probabilities based on the overall survey trend.

9 Conclusion

This thesis has presented a comprehensive sensitivity analysis of the proportional representation system used in the Dutch House of Commons (Tweede Kamer). By evaluating both structural parameters (election thresholds and seat allocation methods) and stochastic uncertainties (vote counting error and voter uncertainty), the research links the gap between theoretical models and the practical realities of the Dutch TK election system. Through a comprehensive analysis of dynamic election threshold, seat allocation algorithm, vote counting error model, voter uncertainty simulation, and election data from polls, some key conclusions were drawn.

Among the Dutch TK25 election, although 27 political parties participated, only about 8 parties were effective. Within the parliament, 15 political parties are represented, but only about 8 are effective. A sensitive area from 1.8% to 2.7%, the number of political parties decreased from 13 to 7. However, the number of effective political parties declined more slowly, remaining at 7 to 8. Therefore, raising the electoral thresholds to eliminate smaller parties will not weaken the power of the major, effective political parties, instead it reduced the fairness of the election. We believe that raising the existing threshold 0.67% will not have a positive impact on the Dutch TK25. For the Dutch Electoral Council (Kiesraad), raising the threshold should be done cautiously, especially in the sensitive area from 1.8% to 2.7%, to prevent the exclusion of minority voices.

Three of the common allocation methods, the Sainte-Laguë Method, Hare Quota Method, and Droop Quota Method, produce an identical distribution of seats when using 0.67% threshold. The D'Hondt Method has an inherent mathematical bias that works against the smaller parties and provides a support to larger parties, producing a relatively lower fairness. Additionally, by testing dynamic thresholds on six different methods shows that different methods did not affect the electoral fairness or the number of effective parliamentary parties of the Dutch TK25. At low thresholds, the D'Hondt method ensures the least degree of parliamentary fragmentation compared to other methods. But it is relatively less effective in ensuring the fairness of elections. As the threshold increases past 2.7%, the differences between all methods almost disappear. Given the low electoral threshold in the Dutch TK, the D'Hondt method is effective in maintaining government stability.

Vote counting errors create a spatial bias on the ballot paper. Large parties lose votes to their smaller physical neighbors, causing their final counts to be underestimated. Conversely, parties located next to large parties receive a boost in their vote. However, these counting errors caused by the layout of the political party on the ballot paper are not large enough to change the overall vote distribution. In the Dutch Tk25, the actual counting error of 7,766 misclassified votes causes no changes to the parliamentary seats. At least 10,000 ballots would need to be misclassified to cause changes in party seats. Even so, compared to the official TK25 election results, this did not have a impact on the distribution of parliamentary seats. The Dutch TK election system is robust against physical vote counting errors. However, voters still complaints about the large ballot paper. We recommend the Dutch Electoral Council (Kiesraad) redesign the ballot, to make it easier for voters to cast their ballots and for vote counters to classify them more clearly.

In the simulation experiment of voter shifts, the centrist ($\mathcal{B}_3$) and progressive-liberal ($\mathcal{B}_2$) blocs lose hundreds of thousands of votes. At the same time, the left-social, market-liberal, and Conservative-right blocs absorb these transferring voters. This finding shows that centrist blocs are typically affected by voters uncertainity. Specifically, voter uncertainty causes major parties, especially CDA and D66, to lose a large amount of votes. These lost votes mostly transfer to smaller, ideologically similar parties within the same political bloc. In the final stages before the election, for parties that are close to the centrist ideology bloc should focus on consolidating their core supporters and strengthening their policies to prevent a loss of voters.

The Dutch TK election poll data from TK23 to TK25 shows that voter volatility was mainly concentrated among major parties such as PVV, CDA, NSC, JA21, D66, and VVD. Especially NSC, which went from large support in TK23 to almost no support in TK25. Smaller parties, such as SGP, CU, DENK, 50PLUS, and Volt, remained relatively stable. At the bloc level, the conservative, right-populist and nationalist bloc ($\mathcal{B}_5$) showed the highest volatility, followed by the Market-liberal and centre-right bloc ($\mathcal{B}_4$) and the Centrist, Christian-democratic and governance bloc ($\mathcal{B}_3$). In contrast, the Left-social and redistributive bloc ($\mathcal{B}_1$) showed lower volatility. The regression analysis shows that as the election approaches, the error between the polls and the actual TK25 election gradually decreases. The model indicates that opinion polls became more accurate when approaching the TK25 election. Therefore, when analyzing or predicting the results of recent elections, poll data closer to election day is more meaningful.

In summary, the Dutch proportional representation system shows strong robustness to changes in seat allocation methods, and vote counting error disturbances. However, it remains sensitive to high uncertainty among voters and changes in election thresholds. This thesis provides a framework for evaluating electoral stability. These analytical methods offer a foundation for future political election research.

References

[1] Kees Aarts and Jacques Thomassen. "Dutch Voters and the Changing Party Space 1989–2006". In: *Acta Politica* 43.2 (July 1, 2008), pp. 203–234. ISSN: 1741-1416. DOI: 10.1057/ap.2008.6. URL: https://doi.org/10.1057/ap.2008.6 (visited on 06/27/2026).

[2] Universiteit van Amsterdam. *De Nederlandse kiezer: beweeglijk, maar niet willekeurig.* Universiteit van Amsterdam. June 3, 2026. URL: https://www.uva.nl/content/nieuws/persberichten/2026/06/de-nederlandse-kiezer-beweeglijk-maar-niet-willekeurig.html (visited on 06/17/2026).

[3] Stephen Ansolabehere and Charles Stewart. "Residual Votes Attributable to Technology". In: *The Journal of Politics* 67.2 (May 2005), pp. 365–389. ISSN: 0022-3816, 1468-2508. DOI: 10.1111/j.1468-2508.2005.00321.x. URL: https://www.journals.uchicago.edu/doi/10.1111/j.1468-2508.2005.00321.x (visited on 06/27/2026).

[4] Asher. *Ipsos I&O-zetelpeiling: CDA levert in, partijen groeien naar elkaar toe.* Ipsos I&O Publiek. Oct. 25, 2025. URL: https://www.ipsos-publiek.nl/actueel/ipsos-io-zetelpeiling-cda-levert-in-partijen-groeien-naar-elkaar-toe/ (visited on 06/17/2026).

[5] Damien Bol, Jean-Benoit Pilet, and Pedro Riera. "The international diffusion of electoral systems: The spread of mechanisms tempering proportional representation across Europe". In: *European Journal of Political Research* 54.2 (May 2015), pp. 384–410. ISSN: 0304-4130, 1475-6765. DOI: 10.1111/1475-6765.12091. URL: https://www.cambridge.org/core/journals/european-journal-of-political-research/article/abs/international-diffusion-of-electoral-systems-the-spread-of-mechanisms-tempering-proportional-representation-across-europe/DD40D40D76A007BC26186798140D24E5#access-block (visited on 06/27/2026).

[6] *Dutch Abandon Voting Software Amid Hacking Fears.* Mar. 6, 2017. URL: https://www.newsweek.com/dutch-election-electronic-voting-hacking-russia-france-macron-trump-clinton-564198 (visited on 05/07/2026).

[7] L. van Eck, S. E. Visagie, and H. C. de Kock. "Fairness of seat allocation methods in proportional representation". In: *ORiON* 21.2 (2005), pp. 93–110. ISSN: 2224-0004. URL: https://www.ajol.info/index.php/orion/article/view/34253 (visited on 03/31/2026).

[8] Albert Falcó-Gimeno and Indridi H. Indridason. "Uncertainty, Complexity, and Gamson's Law: Comparing Coalition Formation in Western Europe". In: *West European Politics* 36.1 (Jan. 1, 2013), pp. 221–247. ISSN: 0140-2382. DOI: 10.1080/01402382.2013.742758. URL: https://doi.org/10.1080/01402382.2013.742758 (visited on 05/07/2026).

[9] Jarosław Flis, Wojciech Słomczyński, and Dariusz Stolicki. "Pot and ladle: a formula for estimating the distribution of seats under the Jefferson–D'Hondt method". In: *Public Choice* 182.1 (Jan. 1, 2020), pp. 201–227. ISSN: 1573-7101. DOI: 10.1007/s11127-019-00680-w. URL: https://doi.org/10.1007/s11127-019-00680-w (visited on 06/27/2026).

[10] Michael Gallagher. "Proportionality, disproportionality and electoral systems". In: *Electoral Studies* 10.1 (Mar. 1, 1991), pp. 33–51. ISSN: 0261-3794. DOI: 10.1016/0261-3794(91)90004-C. URL: https://www.sciencedirect.com/science/article/pii/026137949190004C (visited on 06/24/2026).

[11] William A. Gamson. "A Theory of Coalition Formation". In: *American Sociological Review* 26.3 (1961), pp. 373–382. ISSN: 0003-1224. DOI: 10.2307/2090664. URL: https://www.jstor.org/stable/2090664 (visited on 05/07/2026).

[12] Stephen N. Goggin, Michael D. Byrne, and Juan E. Gilbert. "Post-Election Auditing: Effects of Procedure and Ballot Type on Manual Counting Accuracy, Efficiency, and Auditor Satisfaction and Confidence". In: *Election Law Journal: Rules, Politics, and Policy* 11.1 (Mar. 1, 2012), pp. 36–51. ISSN: 1533-1296. DOI: 10.1089/elj.2010.0098. URL: https://doi.org/10.1089/elj.2010.0098 (visited on 06/27/2026).

[13] E. Harteveld et al. *Dutch Parliamentary Election Study 2025 (DPES/NKO 2025)*. June 2, 2026. DOI: 10.17026/SS/ZBNO8O. URL: https://ssh.datastations.nl/dataset.xhtml?persistentId=doi:10.17026/SS/ZBNO8O (visited on 06/17/2026).

[14] *Ipsos I&O Publiek - Toonaangevend onderzoek in de publieke sector*. Ipsos I&O Publiek. URL: https://www.ipsos-publiek.nl/ (visited on 06/03/2026).

[15] Will Jennings and Christopher Wlezien. "Election polling errors across time and space". In: *Nature Human Behaviour* 2.4 (Apr. 2018), pp. 276–283. ISSN: 2397-3374. DOI: 10.1038/s41562-018-0315-6. URL: https://www.nature.com/articles/s41562-018-0315-6 (visited on 06/27/2026).

[16] Kiesraad. *27 partijen nemen deel aan Tweede Kamerverkiezing | Kiesraad.nl*. Last Modified: 2025-09-29T12:22:41.528Z. Sept. 19, 2025. URL: https://www.kiesraad.nl/actueel/nieuws/2025/09/19/27-partijen-nemen-deel-aan-tweede-kamerverkiezing (visited on 06/15/2026).

[17] Kiesraad. *Data-analyse verkiezingsuitslagen Tweede Kamerverkiezing 2025 | Kiesraad.nl*. Last Modified: 2026-03-02T16:34:32.332Z. Mar. 3, 2026. URL: https://www.kiesraad.nl/documenten/2026/03/03/data-analyse-verkiezingsuitslagen-tweede-kamerverkiezing-2025 (visited on 06/15/2026).

[18] Kiesraad. *Organisatie stemming en telling | Kiesraad.nl.* Last Modified: 2025-11-03T12:32:51.713Z. Jan. 15, 2025. URL: https://www.kiesraad.nl/verkiezingen/tweede-kamer/documenten-tweede-kamerverkiezing-2025/organisatie-stemming-en-telling-tk25 (visited on 06/13/2026).

[19] Markku Laakso and Rein Taagepera. "“Effective” Number of Parties". In: *Comparative Political Studies* 12.1 (Apr. 1, 1979), pp. 3–27. ISSN: 0010-4140. DOI: 10.1177/001041407901200101. URL: https://escholarship.org/uc/item/703827nv (visited on 06/16/2026).

[20] *Links en rechts | Parlement.com.* URL: https://www.parlement.com/links-en-rechts (visited on 06/17/2026).

[21] Lanny W. Martin and Randolph T. Stevenson. "Government Formation in Parliamentary Democracies". In: *American Journal of Political Science* 45.1 (2001), pp. 33–50. ISSN: 0092-5853. DOI: 10.2307/2669358. URL: https://www.jstor.org/stable/2669358 (visited on 05/07/2026).

[22] Robin Pascoe. *More councils to use smaller ballot in local elections trial.* DutchNews.nl. Dec. 12, 2025. URL: https://www.dutchnews.nl/2025/12/more-councils-to-use-smaller-ballot-in-local-elections-trial/ (visited on 06/13/2026).

[23] *Proportional Representation Is Breaking Dutch Democracy.* Social Europe. Mar. 20, 2026. URL: https://www.socialeurope.eu/proportional-representation-is-breaking-dutch-democracy (visited on 04/01/2026).

[24] Friedrich Pukelsheim. *Proportional Representation.* Cham: Springer International Publishing, 2017. ISBN: 978-3-319-64706-7 978-3-319-64707-4. DOI: 10.1007/978-3-319-64707-4. URL: http://link.springer.com/10.1007/978-3-319-64707-4 (visited on 06/27/2026).

[25] A. Sainte-Laguë. "La représentation proportionnelle et la méthode des moindres carrés". In: *Annales scientifiques de l'École Normale Supérieure* 27 (1910), pp. 529–542. ISSN: 1873-2151. DOI: 10.24033/asens.627. URL: https://www.numdam.org/item/?id=ASENS_1910_3_27__529_0 (visited on 06/16/2026).

[26] *Tweede Kamer - 29 oktober 2025 - Verkiezingsuitslagen.* URL: https://www.verkiezingsuitslagen.nl/verkiezingen/detail/TK20251029 (visited on 05/07/2026).

[27] Tom Wg Van Der Meer et al. "Are volatile voters erratic, whimsical or seriously picky? A panel study of 58 waves into the nature of electoral volatility (The Netherlands 2006–2010)". In: *Party Politics* 21.1 (Jan. 2015), pp. 100–114. ISSN: 1354-0688, 1460-3683. DOI: 10.1177/1354068812472570. URL: https://journals.sagepub.com/doi/10.1177/1354068812472570 (visited on 06/27/2026).

Appendix

A. Declaration of AI Usage

During the preparation of this thesis, the author used Google Gemini, Grammarly, DeepL and Gand GitHub Copilot in the following way: Grammarly and DeepL were used for language editing, correcting grammar. Google Gemini was used for improving the clarity of the academic writing, and assisting with LaTeX formatting. GitHub Copilot was used to assist with finding and solving bugs in the Python code. The author takes full responsibility for the content of the work.

B. Data and Code Availability

The complete Python implementation of the numerical simulations, data aggregation, and visualization scripts used in this thesis are publicly available on GitHub. The source code and dataset can be accessed at: `https://github.com/SZhang666/Thesis_SZhang/releases/tag/Thesis`

C. List of Symbols

Symbols used in Section 3

$\mathcal{P}$	Set of participating parties, where $\mathcal{P} = \{1, 2, \ldots, n\}$.
$\mathcal{V}_i$	Percentage of votes received by party i.
$\mathcal{S}_i$	Percentage of seats allocated to party i.
$ENPV$	Effective Number of Electoral Parties.
$ENPP$	Effective Number of Parliamentary Parties.
LSq	Gallagher Index

Symbols used in Section 4

V_i	Valid votes received by party i.
V_{total}	Total valid votes cast in the election.
S	Total fixed parliamentary seats.
Q	Standard electoral quota.
$s_{base,i}$	Baseline number of initial seats.
s_i	Absolute number of seats.
S_{slack}	Unallocated slack seats.
Q_i	Iterative quotient in Highest Averages (Diviosr) Methods.
Q_{Hare}	The Hare Quota
Q_{Droop}	The Droop Quota
$Q_{Imperiali}$	The Imperiali Quota
R_i	Remainder of votes in Largest Remainder (Quota) Methods.
$S_{initial}$	Initial seats allocated in the first phase.
N_{gov}	Minimum number of parties required to form a majority government.
N_{final}	Final number of parliamentary parties.

voter uncertainty

Symbols used in Section 5

X	Real (error-free) voting vector $[X_{\mathcal{P}}, x_B, x_I]^T$.
$X_{\mathcal{P}}$	The real valid party votes vector $[x_1, x_2, ..., x_n]^T$.
Y	Observed (official) voting vector $[Y_{\mathcal{P}}, y_B, y_I]^T$.
$Y_{\mathcal{P}}$	The observed valid party votes vector $[y_1, y_2, ..., y_n]^T$.
x_j, y_j	True (error-free) and observed votes for party j.
x_B, x_I	True (error-free) blank and invalid ballots.
y_B, y_I	Observed (official) counts for blank and invalid ballots.
ϵ	Total misclassification rate for valid party votes.
$\epsilon_{\mathcal{P}}, \epsilon_B, \epsilon_I$	Error rates of valid votes misclassified to a neighbouring party, blank ballot, or invalid ballot.
ζ	Total misclassification rate for blank votes.
$\zeta_{\mathcal{P}}$, ζ_I	Error rates of blank votes misclassified to a valid party or invalid ballot.

η	Total misclassification rates for invalid votes.
$\eta_{\mathcal{P}}$, η_B	Error rates of invalid votes misclassified to a valid party or blank ballot)
p_j	T Probability of party j's vote shifting to the left adjacent party.
$E_{\mathcal{P},j}$	The event that a counting error occurs for a single valid ballot of party j.
L, R	The events of a ballot shifting to its left or right neighbor.
$V^{(j)}$	The final destinations of the true votes of party j.
w_j	Weight of party j's.
$T(X)$	Transition matrix for the counting error model.
$V_{total(x)}$, $V_{total(y)}$	The sum of the true votes and observed votes.
C	The blank and invalid inflow constant.
M	The reduced linear estimation matrix.
$\hat{X}$	Estimator for the true error-free vote counts.
Σ_Y, Σ_X	The covariance matrices.
Δ_i	Estimated bias $(\hat{x}_i - y_i)$ for party i.
Let σ_i	Standard deviation.
$\hat{\cdot}$	Estimator.

Symbols used in Section 6

$\mathcal{B}_k$	The k-th political bloc.
$Z_{\mathcal{P}}$	Simulated vote vector.
A	Potential voter transfer transition matrix.
α_k	Proportion of voters in bloc k who are uncertain.
β_k	Proportion of uncertain voters in bloc k who move to a different bloc.
p_k	Probability of cross-bloc switchers moving to the adjacent left bloc $(k-1)$.
$\omega_{i,k}$	Weight of party i within its bloc k.
$Z_{i,j}$	The number of voters originally supporting party i finally vote for party j.
R	Total number of Monte Carlo simulation iterations.

Symbols used in Section 7

$V_{i,t}$	Vote share of party i in the t-th public opinion poll.
σ_i^{vote}	Standard deviation (volatility) of the polling vote share for party i.
R_i^{vote}	Range of the polling vote share for party i.
V_i^{TK25}	Actual vote share of party i in the official TK25 election.
MAE_t^{vote}	Mean absolute vote share error for the t-th poll.
d_t	Number of days remaining between the t-th poll and the election day.
β_0	Intercept.
β_1	Slope.
ϵ_t	Random error.
$\bar{\cdot}$	Sample mean.